Computational Materials Science 136 (2017) 280–296

Contents lists available at ScienceDirect

Computational Materials Science

journal homepage: www.elsevier.com/locate/commatsci

Modeling of the bivariate molecular weight distribution-copolymer composition distribution in RAFT copolymerization using probability generating functions

Cecilia Fortunatti *, Claudia Sarmoria, Adriana Brandolin, Mariano Asteasuain

Planta Piloto de Ingeniería Química (PLAPIQUI), Universidad Nacional del Sur (UNS)-CONICET, Camino La Carrindanga km 7, 8000 Bahía Blanca, Argentina

ARTICLE INFO

Article history:
Received 22 December 2016
Received in revised form 10 April 2017
Accepted 12 April 2017

Keywords:
Modeling
Molecular weight distribution (MWD)
Reversible addition fragmentation chain transfer (RAFT)
Probability generating function (pgf)
Copolymerization

ABSTRACT

In this work, we develop a mathematical model of a RAFT copolymerization process able to predict average molecular properties as well as the full bivariate molecular weight distribution – copolymer composition distribution (MWD-CCD) of the copolymer. This model takes into account the three main kinetic theories proposed in the literature. The bivariate MWD-CCD is obtained by means of the 2D probability generating function (pgf) technique. This modeling technique can be used without any simplifying assumptions or a priori knowledge of the distribution shape. The results highlight the advantages of simulation as a powerful tool to get insight in the relationship between operating conditions and molecular structure.

1. Introduction

Reversible addition-fragmentation chain transfer (RAFT) polymerization has enormous potential for scientific and industrial developments. Although the moiety used as mediator for these processes may cause odor and discoloration in the product [1], the effectiveness in achieving the living/controlled behavior and the wide range of polymerizable monomers make this controlled radical polymerization (CRP) technique one of the most promising approaches for the production of tailor-made materials [2].

In RAFT processes, the growth of polymer chains is controlled through the addition of a chain transfer agent (CTA), the RAFT agent, which distributes active radical sites among a large number of chains [3,4]. Through bimolecular transfer processes, a small number of living radicals undergoes chain exchange reactions. These reactions involve the addition of a new radical to a dormant species to form a two-arm intermediate adduct, and the subsequent fragmentation of this species. In this way an equilibrium among the radicals and the dormant species is created [5]: in the pre-equilibrium stage, the RAFT agent adds a propagating radical to produce the two-arm intermediate, which fragments later to liberate either that same radical or a new one, both able to continue with the propagation or termination reactions. When the main equilibrium is reached the two arms of the adduct possess approximately the same number of monomer units, since the growth of all chains proceeds at the same speed on average [6]. It is clear that good control over chain growth requires the exchange reactions to be fast compared with the propagation step [2].

There exists an ongoing debate regarding the kinetics of this process, since some experimental findings indicate that the RAFT moiety does not act as an ordinary chain transfer agent in some cases [7,8]. For RAFT agents such as dithiobenzoates and some dithiocarbamates, an induction period and a retardation of the propagation rate are observed when the CTA concentration is increased. In consequence, different kinetic theories were developed in an effort to properly describe the mechanism of RAFT processes. The slow fragmentation theory (SF) proposed by Barner-Kowollik et al. [9] assumes that the intermediate radical of two arms is relatively stable and fragments slowly. This theory yields good predictions of the rate retardation, but those of the overall radical concentrations were well above the ones experimentally found. In view of these results, Monteiro and de Brouwer [10] proposed that the rate retardation was due to the cross termination of the two-arm adduct with the active radicals instead, giving rise to the intermediate radical termination theory (IRT). This theory could not explain all observations either, since it predicts concentrations of the three-arm star polymer that results from

* Corresponding author.
E-mail addresses: cfortunatti@plapiqui.edu.ar (C. Fortunatti), csarmoria@plapiqui.edu.ar (C. Sarmoria), abrandolin@plapiqui.edu.ar (A. Brandolin), masteasuain@plapiqui.edu.ar (M. Asteasuain).

http://dx.doi.org/10.1016/j.commatsci.2017.04.013
0927-0256/

the cross-termination of the two-arm adduct which are much higher than the ones actually measured. To overcome this difference between theoretical predictions and experimental data, Konkolewicz et al. [11–13] proposed the intermediate radical termination with oligomers theory (IRTO). According to this theory, the two-arm adduct may cross-terminate but only with oligomeric radicals up to two monomers in length, adducing steric hindrance of larger radicals to reach the active center. When these three theories have been used to fit experimental data using the kinetic constants as adjustable parameters, constants with a difference of up to six orders of magnitude were found [14]. Therefore, the kinetic mechanism by which the RAFT process takes place is not fully elucidated. Other approaches with more complex reaction schemes have been presented, such as the so called "missing steps" theory proposed by Buback et al. [15]. According to this theory, the three-arm stars resulting from the cross termination reactions may undergo secondary reactions where the third branch reacts with propagating radicals. Since the phenomena of inhibition and retardation of the polymerization rate could have important effects on both conversion and reaction time, it may be helpful to have comprehensive models for at least the three main (and simpler) kinetic theories discussed in the literature: SF, IRT, and IRTO.

Several efforts have been made to elucidate which theory is correct with the help of mathematical modeling. Feldermann et al. [16] found that the SF theory provided the best fit to kinetic data of the styrene polymerization mediated by cumyl dithiobenzoate. In contrast, Monteiro [17] showed that the IRT was the appropriate theory to model the polymerization of styrene mediated by a polystyryl dithiobenzoate. This was supported by Kwak et al. [18] that obtained experimental evidence of the three-arms products of cross termination reactions. However, Brown et al. [19] suggested that the rate retardation is produced either by the SF or IRTO mechanisms. They found no evidence of three-arm polymer products in the polymerization of styrene mediated by benzyl-9H-carbazole-9-carbodithioate and their IRTO model fitted well the experimental data. Ting et al. [20] also found experimental evidence in support of the IRTO theory. Suzuki et al. [21] carried out miniemulsion polymerization experiments that when analyzed on a theoretical base indicated that the bimolecular termination between the two-arms adduct and propagating radicals is the most important reason for rate retardation. However, they did not differentiate whether the cross-termination occurred with short radicals (IRTO) or with all of them (IRT).

Precise modeling studies are useful not only to help gaining insight on the fundamentals of this process but also to determine process conditions appropriate for producing tailor-made materials. However, modeling efforts are complicated by the existence of the two-arm intermediate in any of the theories, making necessary the modeling of bivariate molecular weight distributions even for homopolymerization reactions [22].

To the best of our knowledge, theoretical studies on RAFT copolymerization systems [23–32] do not include the prediction of the full molecular weight distribution (MWD). Most of them rely on the method of moments. Monteiro [32] used the method of moments to study a RAFT copolymerization process reaching useful insights regarding the formation of block copolymers. The author assumed that the RAFT moiety acted as an ordinary chain transfer agent. Wang et al. [23] modeled the mechanism of branching and gelation of a RAFT copolymerization system using this approach. Zargar and Schork [24] also used the balances of moments to assess the effect of variation of process conditions on the size of monomer sequences. Even more complex mechanisms, such as hyperbranching RAFT copolymerization, have been studied with the use of this technique [25]. Salami-Kalajahi et al. [26] used the method of moments to fit the experimental data of styrene-butyl acrylate RAFT copolymerization reported by Sun et al. [30]. They obtained an excellent agreement of average properties and radical concentration using a complex kinetic mechanism with several parameters. Hlalele et al. [33] implemented a mathematical model in PREDICI of the emulsion copolymerization of butadiene and acrylonitrile. The system was studied both theoretically and experimentally. They compared different experimental protocols and identified trends, but they did not find a good agreement in the number average molecular weight. They alleged unconsidered ramification reactions to explain this disagreement.

Monte Carlo stochastic methods for modeling RAFT copolymerization have been used less frequently than deterministic methods. To the best of our knowledge, Monte Carlo algorithms have been barely used to simulate the production of RAFT copolymers. For instance, Ganjeh-Anzabi et al. [27] successfully simulated a RAFT copolymerization system using a Monte Carlo simulation after fitting of experimental data of molecular weights and conversion for RAFT homopolymerizations.

Models based on the method of moments have been used for the optimization of RAFT copolymerization systems. For instance, Wang et al. [28] developed a theoretical analysis in which they focused on finding optimal operating policies for the synthesis of copolymers with different molecular structures. A model based on the method of moments was employed in this work, and comonomers with different reactivity ratios were considered. Similarly, Ye and Schork [29] optimized a RAFT copolymerization process aiming at obtaining constant composition or linear gradient composition copolymers. In a more comprehensive study, Sun et al. [30] developed a model based on the method of moments and balances of monomer sequences to manipulate the composition of styrene-butyl acrylate RAFT copolymers. They continuously fed comonomer to the reactor according to a programmed feeding rate controlled by a computer and found that the synthesized products had the targeted composition. In later works, the same authors [31] used the developed model to find the feeding policies necessary to obtain several other controlled structures. Using these policies, they were able to synthesize copolymers with the targeted composition and molecular weight. These studies show that modeling and optimization of RAFT polymerization systems is an important tool for obtaining polymers with pre-specified molecular structures.

In the case of RAFT homopolymerizations, works dealing with the prediction of the full (univariate) MWD of the polymer have been reported. For instance, Johnston-Hall and Monteiro [34] modeled the full MWD of poly(methyl methacrylate) mediated by 2-cyanoprop-2-yl dithiobenzoate. Whenever possible, they solved the mass balance equations by direct integration. However, due to the high computational cost of this method, they assumed the shape of the distribution when systems of higher molecular weights were modeled. Konkolewicz et al. [11] obtained a good fit of the MWD by assuming the shape of the distribution. In another paper [12], they validated the proposed mechanism using assumptions such as linear growth of molecular weight with conversion. Later, the same authors used a simpler version of their model to successfully fit the experimental MWD of RAFT oligomers [13].

Zapata-González et al. [22,35] performed a thorough theoretical study of RAFT homopolymerization processes using a model able to describe the reacting medium for the three main kinetic schemes discussed in the literature. The full MWD was obtained by direct integration of the mass balances applying the quasi-steady-state approximation to eliminate the stiffness of the differential equation system. In this way, the use of computational resources was considerably reduced. Barner-Kowollik et al. [36] obtained the full distribution of RAFT polymers using the PREDICI commercial software. This method proved to be capable of properly describing the SF kinetics. Reasonable agreement of the simu-

lated MWD with experimental data was also found. Furthermore, Chaffey-Millar et al. [37] used PREDICI to describe the reaction kinetics of the individual arms of star polymers synthesized by RAFT. The MWDs obtained for each branch were later processed to obtain the full MWD of multi-arm star polymers in a simple and much easier way than modeling straightforwardly the complete distribution. This study gave rise to a series of recommendations that were found very useful by Barner-Kowollik et al. [38] in the synthesis of RAFT star polymers. Jung and Gomes [39] developed a mathematical model assuming that the cumulative MWD follows the normal distribution function. The model output fitted well the real MWD obtained for RAFT miniemulsion polymerization. However, the need of assuming the shape of the distribution is a limitation for modeling other systems.

Monte Carlo methods have also been successfully employed to model the MWD of RAFT homopolymers. Drache et al. [40] used a Monte Carlo approach to obtain the full MWD of poly(methyl methacrylate) obtained via RAFT with cumyl dithiobenzoate as chain transfer agent after fitting the model to experimental data of conversion and average molecular weights [40]. On the other hand, Chaffey-Millar et al. [41] developed a parallelized Monte Carlo method that competes very favorably with PREDICI in terms of speed. This algorithm was not only able to obtain the full MWD of RAFT polymers but also to provide very detailed information on the molecular structure. Pintos et al. [42] implemented a Monte Carlo algorithm of a RAFT homopolymerization system in the open-source programming language called Julia. The model was developed for the SF, IRT and IRTO theories and predicts the full MWD of the polymer as well as average molecular properties. Very fast simulation times were achieved.

To the extent of our knowledge no reported articles have dealt with the obtainment of the full bivariate MWD-CCD of RAFT copolymers.

In previous works, we have presented a mathematical model for RAFT homopolymerizations capable of dealing with the three main kinetic mechanisms [6,43]. This model is able to predict not only the average properties and the full MWD of the overall polymer but also the full bivariate distribution of the two-arm adduct, giving a significant level of detail of the reacting medium of these complex processes. The prediction of the univariate and bivariate MWDs, made by means of probability generating functions (pgf), proved to be accurate and efficient [6]. In the present work, the above model is extended to address the RAFT copolymerization. The prediction of the bivariate MWD-CCD is included in the model. The copolymerization of styrene (St) and methyl methacrylate (MMA) mediated by cumyl phenyl-dithioacetate is considered as a case study. The results highlight the potential of simulation to help in the design of unique materials with properties specified beforehand through the manipulation of process conditions.

2. Methods

2.1. Case study

The comprehensive model presented in this work can be applied to different RAFT copolymerization systems by appropriate selection of kinetic parameters. To show the model capabilities the following case study was selected: bulk copolymerization of styrene and methyl methacrylate (St = M_A and MMA = M_B) mediated by cumyl phenyl-dithioacetate, using 2,2-azobis(isobutyronitrile) (AIBN) as initiator. This copolymer has both technological and scientific interest. Block copolymers of poly(St-*co*-MMA) have been extensively studied for the production of nanoscale patterns thanks to their ability to maintain the same morphological arrangement through the entire material and the ease of removal of the MMA block by means of UV exposure [44]. Besides, gradient copolymers, which for most comonomer pairs can only be prepared with a CRP technique, may have a better performance in some applications thanks to their ability to form broader interphase regions. Although the advantages of gradient copolymers over conventional compatibilizer systems have not been demonstrated up to now, it was proved that poly(St-*grad*-MMA) can effectively act as blend stabilizer in poly(styrene)/poly(methylmethacrylate) and poly(vinyl-chloride)/poly(styrene-butadienes tyrene) blends [45]. The RAFT technology is a suitable means of synthesizing St-MMA copolymers with controlled structure. In previous works [46] we dealt with the study of copolymerization of St and MMA by nitroxide mediated polymerization (NMP). Now we wish to extend this analysis to the synthesis of this copolymer by RAFT polymerization.

2.2. Mathematical modeling

A mathematical model based on population balances was developed for the RAFT copolymerization process, keeping in mind the objective of predicting average molecular properties as well as the full MWD-CCD of both the overall copolymer and the two-arm adduct.

First, a proper kinetic mechanism was selected. Then, mass balances for each of the reactive species were posed for batch and semibatch reactors. The system was transformed to reduce its size by means of the well-known method of moments (to predict average molecular properties) and the 2D pgf transformation technique (to deal with distributed molecular properties). For this purpose, proper definitions for double order moments and 2D pgfs were employed. Details on each step are given in the following subsections.

2.3. Kinetic mechanism

The kinetic mechanism of the RAFT copolymerization that is considered is as follows (where superscripts i, j or k = A or B):

$$\text{Initiation}: \quad \begin{aligned} &I \xrightarrow{f\ k_d} 2I^{\cdot} \\ &I^{\cdot} + M_A \longrightarrow R^A_{1,0} \\ &I^{\cdot} + M_B \longrightarrow R^B_{0,1} \end{aligned} \tag{1}$$

$$\text{Thermal initiation of styrene}: \quad 3M_A \xrightarrow{k_{th}} R^A_{1,0} + R^A_{2,0} \tag{2}$$

$$\text{Propagation}: \quad \begin{aligned} &R^i_{n,s} + M_A \xrightarrow{k_{p,iA}} R^A_{n+1,s} \\ &R^i_{n,s} + M_B \xrightarrow{k_{p,iB}} R^B_{n,s+1} \end{aligned} \tag{3}$$

Chain termination

$$\text{by combination}: \quad R^i_{n,s} + R^j_{g,h} \xrightarrow{k_{tc,ij}} P_{n+g,s+h} \tag{4}$$

$$\text{by disproportionation}: \quad R^i_{n,s} + R^j_{g,h} \xrightarrow{k_{td,ij}} P_{n,s} + P_{g,h} \tag{5}$$

$$\text{Chain transfer to monomer}: \quad \begin{aligned} &R^i_{n,s} + M_j \xrightarrow{k_{trm,ij}} P_{n,s} + R^j_{a,b} \\ &\text{with } a,b = \begin{cases} 1,0 & \text{if } j = A \\ 0,1 & \text{if } j = B \end{cases} \end{aligned} \tag{6}$$

RAFT pre-equilibrium

$$\text{Addition}: \quad R^i_{n,s} + TR_0 \xrightarrow{k^0_{a\,i}} R^i_{n,s}TR_0 \tag{7}$$

$$\text{Fragmentation}: \quad \begin{aligned} &R^i_{n,s}TR_0 \xrightarrow{(1/2)\ k^0_{f\,i}} TR^i_{n,s} + R_{0,0} \\ &R^i_{n,s}TR_0 \xrightarrow{(1/2)\ k^0_{f\,i}} TR_0 + R^i_{n,s} \end{aligned} \tag{8}$$

RAFT core equilibrium

$$\text{Addition}: \quad R^i_{n,s} + TR^j_{g,h} \xrightarrow{k_{a\,i}} R^i_{n,s}TR^j_{g,h} \tag{9}$$

$$\text{Fragmentation}: \quad \begin{aligned} &R^i_{n,s}TR^j_{g,h} \xrightarrow{(1/2)\ k_{f\,i}} R^i_{n,s} + TR^j_{g,h} \\ &R^i_{n,s}TR^j_{g,h} \xrightarrow{(1/2)\ k_{f\,j}} TR^i_{n,s} + R^j_{g,h} \end{aligned} \tag{10}$$

Chain termination of RAFT adduct

$$\text{cross-termination}: \quad R^i_{n,s} + R^j_{g,h}TR^k_{m,t} k_{c,i} \xrightarrow{k_{c,i}} P_{n+g+m,s+h+t}$$
$$\text{the length of radical chain is} \begin{cases} \text{IRT}: & n+s=0,\ldots,\infty \\ \text{IRTO}: & n+s=0,1,2 \end{cases} \tag{11}$$

The chemical species involved are: initiator (I), monomers M_A and M_B, active radicals with a monomer i in the chain end, n units of M_A, and s units of M_B ($R^i_{n,s}$), one-arm dormant radicals with M_i in the chain end, n units of M_A, and s units of M_B ($TR^i_{n,s}$), two-arm adduct radicals with n units of M_A and s units of M_B in the branch ended in M_i, and g units of M_A and h units of M_B in the other branch ended in M_j ($R^i_{n,s}TR^j_{g,h}$), RAFT chain transfer agent or CTA (TR_0), and dead polymer with n units of M_A and s units of M_B ($P_{n,s}$). The subscripts n, s, g, h, m and t in the polymeric species may take values from 0 to ∞.

The differences between the kinetic theories SF and IRT/IRTO are taken into account by estimating different values for the rate constants corresponding to the reactions of addition, fragmentation, and cross-termination of the two-arms adduct. The latter reaction is active only for the IRT and IRTO theories. Besides, differences between IRT and IRTO arise in the species that take part in the cross-termination reaction (Eq. (11)), something that leads to different balance equations.

For the case study presented in Section 2.1, the kinetic parameters that do not depend on RAFT specific reactions (reactions (1)–(6) of the kinetic mechanism) were taken from our previous work on NMP of St and MMA [46] and are shown in Table A.1 in Appendix A.2. The kinetic parameters that depend on the RAFT specific reactions (reactions (7)–(11) of the kinetic mechanism) are shown in Table 1. Auxiliary model equations such as the density, average molecular weights, average composition and conversion equations are presented in Appendix A.3.

The selection of the values for the kinetic constants in Table 1 will be discussed below. There is plenty of information about the kinetic rate constants corresponding to the conventional free radical copolymerization of styrene and methyl methacrylate. However, kinetic data for the RAFT copolymerization of these monomers is scarce and not always applicable to the kinetic mechanism considered in this work. For instance, Kubo et al. [47] reported the value of a RAFT transfer reaction constant for the copolymerization of St and MMA, but they considered a fast transfer according to the following reaction:

$$R^i_{n,s} + TR^j_{g,h} \underset{k_{ji}}{\overset{k_{ij}}{\rightleftarrows}} TR^i_{n,s} + R^j_{g,h} \tag{12}$$

This reaction neglects the presence of the intermediate adduct (compare with reactions (7)–(11) of the kinetic mechanism). Therefore, the value of the transfer reaction constant reported by Kubo et al. [47] is not applicable to the more detailed kinetic mechanism considered in the present work.

In view of the lack of data about the kinetic constants for the RAFT copolymerization of St and MMA, values taken from homopolymerization reactions of these monomers were used in the present work for the addition and fragmentation kinetic constants. The constants reported by Barner-Kowollik et al. [9] were used as reference. These authors presented values of the addition and fragmentation rate constants for the RAFT homopolymerizations of St and MMA, both mediated by cumyl phenyldithioacetate using AIBN as initiator. Both experiments were carried out at 60 °C. They obtained the kinetic constants by fitting against experimental data using a model that followed the SF kinetics. Therefore, for the addition and fragmentation constants of the SF model presented in this work the data from Barner-Kowollik et al. [9] were used. In order to use this homopolymerization information in the copolymerization model, it was assumed that the reaction rates of the addition and fragmentation steps are governed solely by the nature of the macroradicals participating in them, as if they were in a homopolymerization reaction. That is, the kinetic constant of the addition reaction of macroradical $R^i_{n,s}$ to the one-arm dormant species $TR^j_{g,h}$ is $k_{a,i}$, regardless the nature of the monomer j in the chain end of the one-arm dormant species (see Eq. (9)). Likewise, the two-arm adduct $R^i_{n,s}TR^j_{g,h}$ fragments with reaction rate proportional to $(1/2)\ k_{f\,i}$ when the product is $R^i_{n,s}$ and $TR^j_{g,h}$, and proportional to $(1/2)\ k_{f\,j}$ when the product is $TR^i_{n,s}$ and $R^j_{g,h}$ (see Eq. (10)).

As no data about the kinetic constants for the system under study was available for the IRT and IRTO theories, the corresponding addition, fragmentation and cross termination constants were tuned so that the model yielded profiles of average molecular weights and composition vs. conversion similar to those of the SF theory. With this purpose, a parameter estimation problem was posed in gPROMS (Process Systems Enterprise, Ltd.) to obtain the required rate constants, constrained within bounds that ensured that the results were of the same order of magnitude of constants reported in the literature for similar copolymerization systems. For simplicity, a single set of constants was used for both the pre-

Table 1
Values of the addition, fragmentation and cross-termination rate constants used for each kinetic theory.

Theory	Parameter		
	Addition ($L\,mol^{-1}\,s^{-1}$)	Fragmentation (s^{-1})	Cross-termination ($L\,mol^{-1}\,s^{-1}$)
SF	$k_{a,A} = k^0_{a,A} = 5.6 \times 10^5$ [9] $k_{a,B} = k^0_{a,B} = 1 \times 10^5$ [9]	$k_{f,A} = k^0_{f,A} = 0.27$ $k_{f,B} = k^0_{f,B} = 0.27$ [9]	$k_{c,A} = k_{c,B} = 0$
IRT	$k_{a,A} = k^0_{a,A} = 8.32 \times 10^6$ $k_{a,B} = k^0_{a,B} = 1.62 \times 10^7$	$k_{f,A} = k^0_{f,A} = 3.82 \times 10^5$ $k_{f,B} = k^0_{f,B} = 2.38 \times 10^6$	$k_{c,A} = 4.12 \times 10^7$ $k_{c,B} = 8.53 \times 10^6$
IRTO	$k_{a,A} = k^0_{a,A} = 2.98 \times 10^4$ $k_{a,B} = k^0_{a,B} = 6.54 \times 10^6$	$k_{f,A} = k^0_{f,A} = 166.7$ $k_{f,B} = k^0_{f,B} = 1348$	$k_{c,A} = 7.1 \times 10^7$ $k_{c,B} = 4.33 \times 10^7$

equilibrium and the core equilibrium (that is, $k^0_{a\ i} = k_{a\ i}$ and $k^0_{f\ i} = k_{f\ i}$).

Modeling studies on the diffusional effects on RAFT polymerization are scarce. Wang and Zhu [48] studied theoretically how the diffusion-controlled reactions affect reaction kinetics and polymer molecular properties. Peklak et al. [49] have found that diffusional effects play an important role when conversions are over 50%. More recently, D'hooge et al. [50] presented a review of the commonly used diffusion models and a large study on how diffusional limitations affects the CRP processes in NMP, ATRP and RAFT polymerizations. Among other important conclusions, they determined that termination reactions were the most affected ones. These studies show that diffusion in controlled polymerization reactions should not be overlooked at high conversions. Since all but one of the simulated reactions in the present work reach conversions lower than 50%, the mathematical model does not include diffusional effects. Work is on the way to extend the present model to include them.

2.4. Mass, moments and pgf balances

The global mass balance for a semibatch reactor is:

$$\frac{d(\rho_{mix}\ V)}{dt} = F \tag{13}$$

where ρ_{mix} is the density of the reactive mixture, V is the reaction volume and F is the feed flowrate with units of [mass/time]. This flowrate is zero when dealing with a batch reactor.

The mass balance for each of the reactive species X is:

$$\frac{d([X]\ V)}{dt} = r_X\ V + \frac{F\ x_X}{PM_X} \tag{14}$$

In this equation x_X is the mass fraction of X in the feed flowrate, PM_X is its molecular weight and r_X is the reaction rate. The X species are the initiator, monomers, active radicals, one-arm dormant radicals, two-arm adduct radicals, the RAFT chain transfer agent and dead polymers molecules. For the sake of brevity, the expressions of r_X as functions of the species presented in the kinetic mechanism, as well for their moments and pgfs, are shown in the Appendix (see Appendix A.1, Eqs. (A.1)–(A.10)).

As the mass balances presented in Eq. (14) for the polymer species (X standing for active radicals, one-arm dormant radicals, two-arm adduct radicals and dead polymers) are intrinsically infinite in number, to be able to calculate average or distributed molecular properties some transformations are useful. The 2D (pgf) technique is employed in this work on the mass balances of the polymer species with two characteristic lengths, namely the number of units of each comonomer in the chain. The technique transforms the corresponding infinite mass balance equations to the 2D pgf domain, giving as a result a finite set of equations for the 2D pgf transform of the bivariate MWD of the copolymer [51]. Since the moments of the macromolecular species appear in the transformation, moment balances must be solved together with pgf balances. These moment balances are obtained using the well-known method of moments.

The pgf technique has several advantages that makes it of special interest for the prediction of polymer properties. In the first place, there is no need to use any simplifying assumptions or have previous knowledge of the shape of the MWD. Moreover, it can deal with complex mechanisms. In addition, the model results in a relatively small number of equations that can be solved in a reasonable time.

With the purpose of applying the 2D pgf transform, moment and pgf definitions are needed to be able to transform the original complete set of mass balances. These definitions are presented below.

2.4.1. Moment definitions

Moment of order a,b (a,b = 0,0; 0,1; 0,2; 1,1; 1,0; 2,0) of active radicals with a final unit of monomer i (i = A, B), n units of M_A and m units of M_B:

$$\lambda^i_{a,b} = \sum_{n=0}^{\infty}\sum_{m=0}^{\infty} n^a\ m^b [R^i_{n,m}] \tag{15}$$

Moment of order a,b (a,b = 0,0; 0,1; 0,2; 1,1; 1,0; 2,0) of one-arm dormant radicals with a final unit of monomer i (i = A, B), n units of M_A and m units of M_B:

$$\mu^i_{a,b} = \sum_{n=0}^{\infty}\sum_{m=0}^{\infty} n^a\ m^b [TR^i_{n,m}] \tag{16}$$

Moment of order a,b (a,b = 0,0; 0,1; 0,2; 1,1; 1,0; 2,0) of dead polymer radicals with n units of M_A and m units of M_B:

$$\varepsilon_{a,b} = \sum_{n=0}^{\infty}\sum_{m=0}^{\infty} n^a\ m^b [P_{n,m}] \tag{17}$$

Moment of order a,b (a,b = 0,0; 0,1; 0,2; 1,1; 1,0; 2,0) of two-arm adduct radicals in pre-equilibrium (one branch with 0 units in length) with a final unit of monomer i (i = A, B), n units of M_A and m units of M_B:

$$\omega^i_{a,b} = \sum_{n=0}^{\infty}\sum_{m=0}^{\infty} n^a\ m^b [R^i_{n,m} TR_0] \tag{18}$$

Moment of order a,b,0,0 (a,b = 0,0; 0,1; 0,2; 1,1; 1,0; 2,0) of two-arm adduct radicals with a final unit of monomer i in the first branch and a final unit of monomer j in the other branch (i, j = A, B):

$$\Gamma^{i,j}_{a,b,0,0} = \sum_{n=0}^{\infty}\sum_{m=0}^{\infty} n^a\ m^b \sum_{g=0}^{\infty}\sum_{h=0}^{\infty} [R^i_{n,m} TR^j_{g,\ h}] \tag{19}$$

Partial moment of order 0,0 of two-arm adduct radicals with a final unit of monomer i in the first branch and a final unit of monomer j in the other branch (i, j = A, B).

$$d\gamma^{i,j}_{n,m} = \sum_{g=0}^{\infty}\sum_{h=0}^{\infty} [R^i_{n,m} TR^j_{g,\ h}] \tag{20}$$

This partial moment quantifies the moles of molecules of the two-arm adduct in which one of the branches has n units of M_A and m units of M_B, regardless of the composition of the other arm. This moment allows taking into account the kinetic steps in which the branch with length (n,m) is involved. In view of the possible combinations of monomers in each branch, it is necessary to consider four partial moments $d\gamma^{AA}_{n,m}, d\gamma^{BB}_{n,m}, d\gamma^{AB}_{n,m}, d\gamma^{BA}_{n,m}$.

Please note that the last two partial moments are not the same, since the first superscript indicates the type of monomer in the chain end of the branch being characterized by the number of units of M_A and M_B.

Moment of order a,b (a,b = 0,0; 0,1; 0,2; 1,1; 1,0; 2,0) of the partial moment of order 0, 0 of two-arm adduct radicals with a final unit of monomer i in the first branch and a final unit of monomer j in the other branch (i, j = A, B):

$$\gamma^{i,j}_{a,b} = \sum_{n=0}^{\infty}\sum_{m=0}^{\infty} n^a\ m^b\ d\gamma^{i,j}_{n,m} = \sum_{n=0}^{\infty}\sum_{m=0}^{\infty} n^a\ m^b \sum_{g=0}^{\infty}\sum_{h=0}^{\infty} [R^i_{n,m} TR^j_{g,\ h}] = \Gamma^{i,j}_{a,b,0,0} \tag{21}$$

As it can be observed in Eq. (21), the moment $\gamma^{i,j}_{a,b}$ is equivalent to the four index moment, $\Gamma^{i,j}_{a,b,0,0}$.

Moment of order a,b (a,b = 0,0; 0,1; 0,2; 1,1; 1,0; 2,0) of the two-arm adduct radicals with a final unit of monomer i in the first branch and a final unit of monomer j in the other branch (i, j = A, B), considering the total number of units of each comonomer in both branches:

$$\theta^{i,j}_{a,b} = \sum_{n=0}^{\infty}\sum_{m=0}^{\infty} n^a m^b [(R^i TR^j)_{n,m}] \tag{22}$$

It is worth noting that when one considers the final monomer units of each branch, three species of two-arm adducts result: two species with both active sites of the same sort, $(R^A TR^A)_{n,m}$ and $(R^B TR^B)_{n,m}$, and the species with active sites of different sort, $(R^A TR^B)_{n,m}$. The resulting balances of moments are also generically represented by Eq. (14) when X represents a moment of any of the macromolecular species present in the reaction medium.

The reaction rate expressions that must be used in the moment balances of the polymeric species may be deduced from the mass balances of the polymeric species (Eqs. (A.1)–(A.10) in the Appendix) by applying the corresponding moment definitions presented before. Although the technique for the derivation of the moment balances is well-known, the algebraic process that is involved becomes complex for this system, in particular for the reaction terms involving the two-arm adduct. This species is described by four internal coordinates (i.e. the number of units of monomers A and B in each of the two arms), which requires defining the four index moment $\Gamma^{i,j}_{a,b,0,0}$ and the two index moments $d\gamma^{i,j}_{n,m}$, $\gamma^{i,j}_{a,b}$ and $\theta^{i,j}_{a,b}$. The resulting reaction rate expressions to be used in moment balances are shown in Appendix A.1 (see Eqs. (A.11)–(A.18)).

Some of the moment values are very useful for calculating average molecular properties (molecular weights, instantaneous and cumulative compositions, etc.), as shown in the Appendix (see Appendix A.3).

2.4.2. Pgf definitions

In order to recover the bivariate MWD of the copolymer the following pgf are required:

Pgf of order 0,0 of active radicals with a final unit of monomer i (i = A, B), n units of M_A *and m units of* M_B:

$$\sigma^i_{0,0} = \sum_{n=0}^{\infty}\sum_{m=0}^{\infty} z^n\, w^m [R^i_{n,m}] \tag{23}$$

The values of the dummy variables *z* and *w* of the pgf are determined by the inversion method.

Pgf of order 0,0 of one-arm dormant radicals with a final unit of monomer i (i = A, B), n units of M_A *and m units of* M_B:

$$\varphi^i_{0,0} = \sum_{n=0}^{\infty}\sum_{m=0}^{\infty} z^n\, w^m [TR^i_{n,m}] \tag{24}$$

Pgf of order 0,0 of dead polymer radicals with n units of M_A *and m units of* M_B:

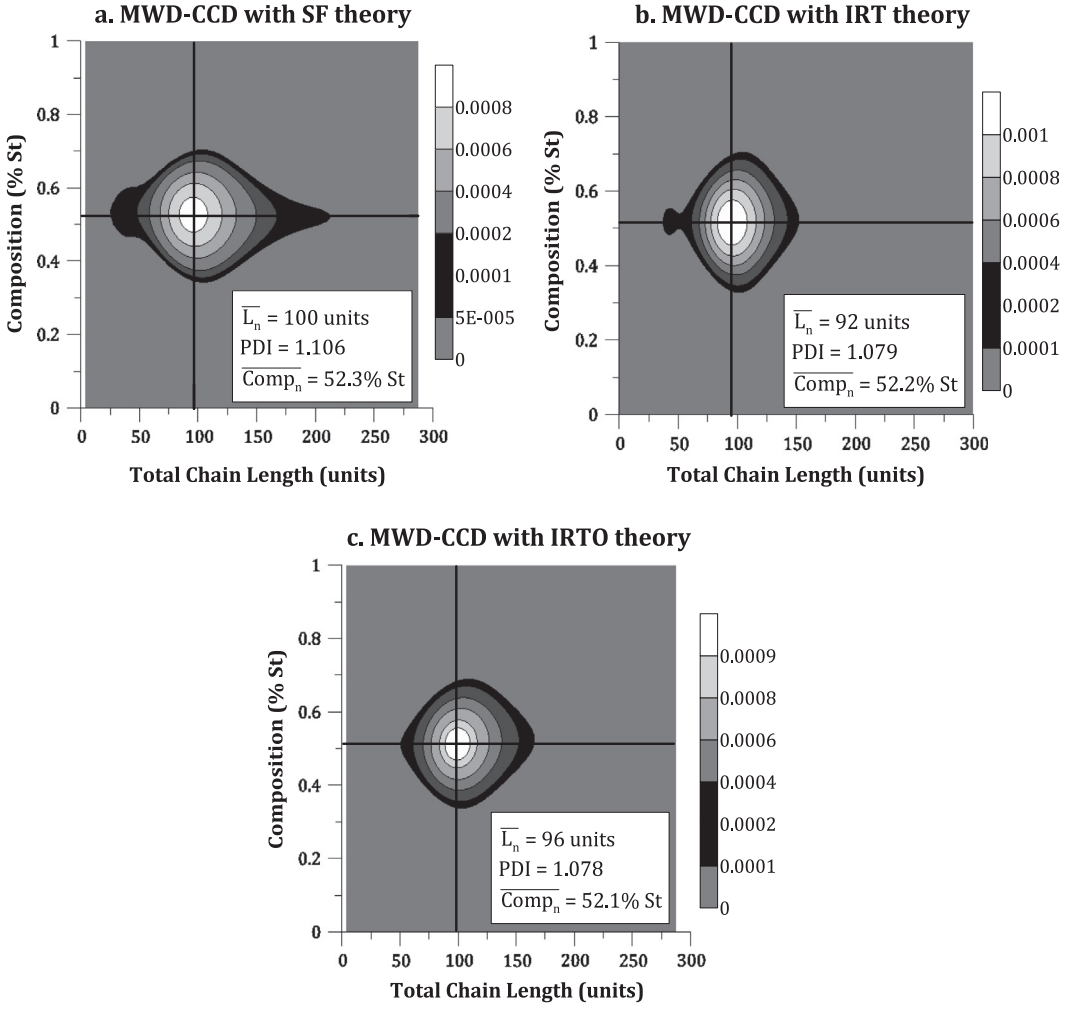

Fig. 1. MMD-CCD of copolymer for the SF, IRT and IRTO theories. Batch operation: t_{final} = 12 h, T = 60 °C, $[St]_0 = [MMA]_0$ = 4.349 mol L^{-1}, $[CTA]_0$ = 0.035 mol L^{-1} and $[I]_0$ = 0.0037 mol L^{-1}.

$$\vartheta_{0,0} = \sum_{n=0}^{\infty}\sum_{m=0}^{\infty} z^n\ w^m [\mathrm{P}_{n,m}] \tag{25}$$

Pgf of order 0,0 of two-arm adduct radicals in pre-equilibrium (one branch with 0 units in length) with a final unit of monomer i (i = A, B), n units of M_A and m units of M_B:

$$\Omega^{i}_{0,0} = \sum_{n=0}^{\infty}\sum_{m=0}^{\infty} z^n\ w^m [\mathrm{R}^{i}_{n,m}\mathrm{TR}_0] \tag{26}$$

Pgf of order 0,0 of the partial 0,0 order moment of two-arm adduct radicals with a final unit of monomer i in the first branch and a final unit of monomer j in the other branch (i, j = A, B):

$$\Upsilon^{i,j}_{0,0} = \sum_{n=0}^{\infty}\sum_{m=0}^{\infty} z^n\ w^m\ d\gamma^{i,j}_{n,m} \tag{27}$$

This pgf is necessary to pose the mass balances that consider reactions of only one of the branches of the two-arm adduct.

Pgf of order 0,0 of the two-arm adduct radicals with a final unit of monomer i in one branch and a final unit of monomer j in the other branch (i, j = A, B), considering the total number of units of each comonomer in both branches:

$$\Theta^{i,j}_{0,0} = \sum_{n=0}^{\infty}\sum_{m=0}^{\infty} z^n\ w^m [(\mathrm{R}^{i}\mathrm{TR}^{j})_{n,m}] \tag{28}$$

The pgf of the overall polymer can be computed from these pgf as follows:

$$\tau_{0,0}(z,w) = \frac{\left\{\begin{array}{c}[\lambda^{\mathrm{A}}_{0,0}\sigma^{\mathrm{A}}_{0,0}(z,w)] + [\lambda^{\mathrm{B}}_{0,0}\sigma^{\mathrm{B}}_{0,0}(z,w)] + \\ [\mu^{\mathrm{A}}_{0,0}\varphi^{\mathrm{A}}_{0,0}(z,w)] + [\mu^{\mathrm{B}}_{0,0}\varphi^{\mathrm{B}}_{0,0}(z,w)] + \\ [\varepsilon_{0,0}\vartheta_{0,0}(z,w)] + [\omega^{\mathrm{A}}_{0,0}\Omega^{\mathrm{A}}_{0,0}(z,w)] + [\omega^{\mathrm{B}}_{0,0}\Omega^{\mathrm{B}}_{0,0}(z,w)] + \\ [\theta^{\mathrm{AA}}_{0,0}\Theta^{\mathrm{AA}}_{0,0}(z,w)] + [\theta^{\mathrm{AB}}_{0,0}\Theta^{\mathrm{AB}}_{0,0}(z,w)] + [\theta^{\mathrm{BB}}_{0,0}\Theta^{\mathrm{BB}}_{0,0}(z,w)]\end{array}\right\}}{\lambda^{\mathrm{A}}_{0,0} + \lambda^{\mathrm{B}}_{0,0} + \mu^{\mathrm{A}}_{0,0} + \mu^{\mathrm{B}}_{0,0} + \varepsilon_{0,0} + \omega^{\mathrm{A}}_{0,0} + \omega^{\mathrm{B}}_{0,0} + \theta^{\mathrm{AA}}_{0,0} + \theta^{\mathrm{AB}}_{0,0} + \theta^{\mathrm{BB}}_{0,0}} \tag{29}$$

The pgf $\tau_{0,0}(z,w)$ is the transform of the bivariate distribution of the global population of polymer species, that is, the sum of active radicals, one-arm dormant radicals, dead polymer and two-arm adduct radicals.

The resulting pgf balances are also generically represented by Eq. (14) when X represents a pgf of any of the macromolecular species present in the reaction medium.

The corresponding reaction rate expressions of the pgf balances may be derived from the mass balances of the polymeric species (Eqs. (A.1)–(A.10) in the Appendix). The required procedure is well described in the literature [51]. However, the reaction terms involving the two-arm adduct introduced a significant complexity that has not been faced in previous reports of the pgf technique. The resulting pgf balances are shown in Appendix A.1 (see Eqs. (A.19)–(A.25)).

2.4.3. Numerical inversion of 2D pgfs

After solving the pgf balances, the resulting pgfs are numerically inverted to recover the bivariate MWD distribution using an appropriate inversion method. A 2D pgf inversion method based on the Papoulis method originally proposed for the inversion of univariate Laplace transforms was used in this paper. Further details about this method may be found elsewhere [52].

All the simulations were performed in gPROMS in a standard desktop computer. The resulting differential algebraic equation system was solved using the proprietary solver DASOLV [53].

3. Results and discussion

3.1. Prediction of the full bivariate MWD-CCD

Numerical inversion of the pgf $\tau_{0,0}(z,w)$ (see Eq. (29)) yields the bivariate MWD of the global population of polymeric species, which is the distribution in terms of the number of units of each comonomer in the chain. Simple post-processing of this distribution allows obtaining the bivariate MWD-CCD of the copolymer. The mathematical model is able to compute the MWD-CCD for any of the three main kinetic mechanisms proposed in the literature for RAFT polymerizations. This can be accomplished in spite of the difficulties associated with the four-dimensional nature of the copolymeric two-arm adduct.

Fig. 1 shows the MWD-CCD obtained with the three theories described in Section 2.3 for a given set of operating conditions. Number average chain length, PDI and cumulative composition ($\overline{Comp_n}$) are reported in the figure. It can be seen that the MWD-CCD are similar for the SF, IRT and IRTO models. This is not surprising because some of the kinetic parameters were tuned so that the average molecular weights and conversions were similar in the three cases. Nevertheless, it can be observed that the distribution predicted by the SF model is slightly broader than the other two in the chain length dimension. This is consistent with the slightly higher PDI predicted by this model.

Note that the MWD-CCD figures have an approximate axial symmetry with respect to a chain length axis and a composition axis, indicated in the figure. These axes are nearly equal to the number average chain-length and to the average composition, respectively. This symmetry means that polymer chains with different chain length (vertical slices) have the same CCD shape, and alternatively that chains with different composition (horizontal slices) have the same MWD shape.

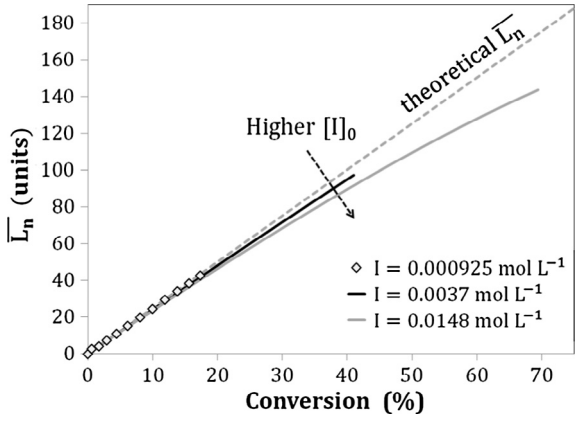

Fig. 2. Number-average chain length for different $[I]_0$ predicted by the model compared with the theoretical value calculated with Eq. (30). Batch operation: t_{final} = 12 h, T = 60 °C, $[St]_0 = [MMA]_0$ = 4.349 mol L^{-1}, $[CTA]_0$ = 0.035 mol L^{-1}.

Table 2
Polymer molecular properties for different $[I]_0$. Batch operation: t_{final} = 12 h, T = 60 °C, $[St]_0 = [MMA]_0$ = 4.349 mol L^{-1}, $[CTA]_0$ = 0.035 mol L^{-1}.

$[I]_0$ (mol L^{-1})	Composition (% St)	$\overline{L_n}$ (units)	PDI	Conversion (%)	Dead chains (w/w %)
0.000925	52.7	47	1.097	19.1	0.8
0.0037	52.3	100	1.106	42.2	4.1
0.0148	51.8	146	1.225	70.6	16.6

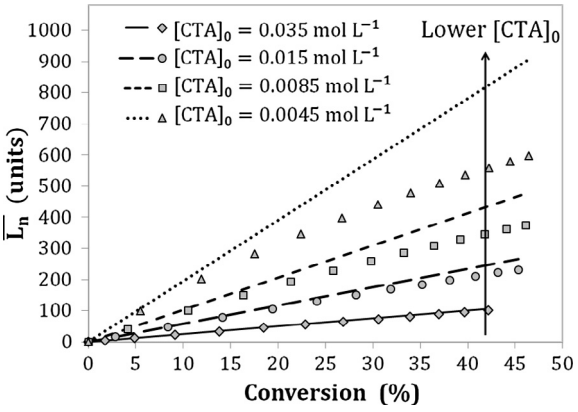

Fig. 3. Number-average chain length for different $[CTA]_0$ (symbols) compared with the theoretical value calculated with Eq. (30) (lines). Batch operation: t_{final} = 12 h, T = 60 °C, $[St]_0 = [MMA]_0$ = 4.349 mol L^{-1}, $[I]_0$ = 0.0037 mol L^{-1}.

A low PDI does not necessarily imply a unimodal MWD [54], so the full distribution can aid to precisely determine the uniformity of the material. Copolymer composition distributions add significant knowledge about the molecular microstructure of chains which can hardly be obtained experimentally [55]. Furthermore, the combined MWD-CCD allows predicting the composition of chains of every size. This information could be of great help for laboratory and industrial practitioners considering the high level of control demanded to fulfill the requirements of some advanced materials. For instance, changes in copolymer composition and the breadth of MWD affects the self-assembly of block copolymers [44] which will ultimately influence the quality of the produced patterns. Therefore, the full MWD-CCD could help to identify defects in the polymer matrix before its production and also provide help in their quantification. In addition, the mathematical model of the process allows obtaining helpful, detailed information about the polymerization rate and polymer structure.

Table 3
Polymer molecular properties for different $[CTA]_0$. Batch operation: t_{final} = 12 h, T = 60 °C, $[St]_0 = [MMA]_0$ = 4.349 mol L^{-1}, $[I]_0$ = 0.0037 mol L^{-1}.

$[CTA]_0$ (mol L^{-1})	Composition (% St)	$\overline{L_n}$ (units)	PDI	Conversion (%)	Dead chains (w/w %)
0.035	52.3	100	1.106	42.2	4.1
0.015	52.2	232	1.152	45.4	10.3
0.0085	52.2	376	1.224	46.1	17.6
0.0045	52.2	598	1.350	46.5	30.1

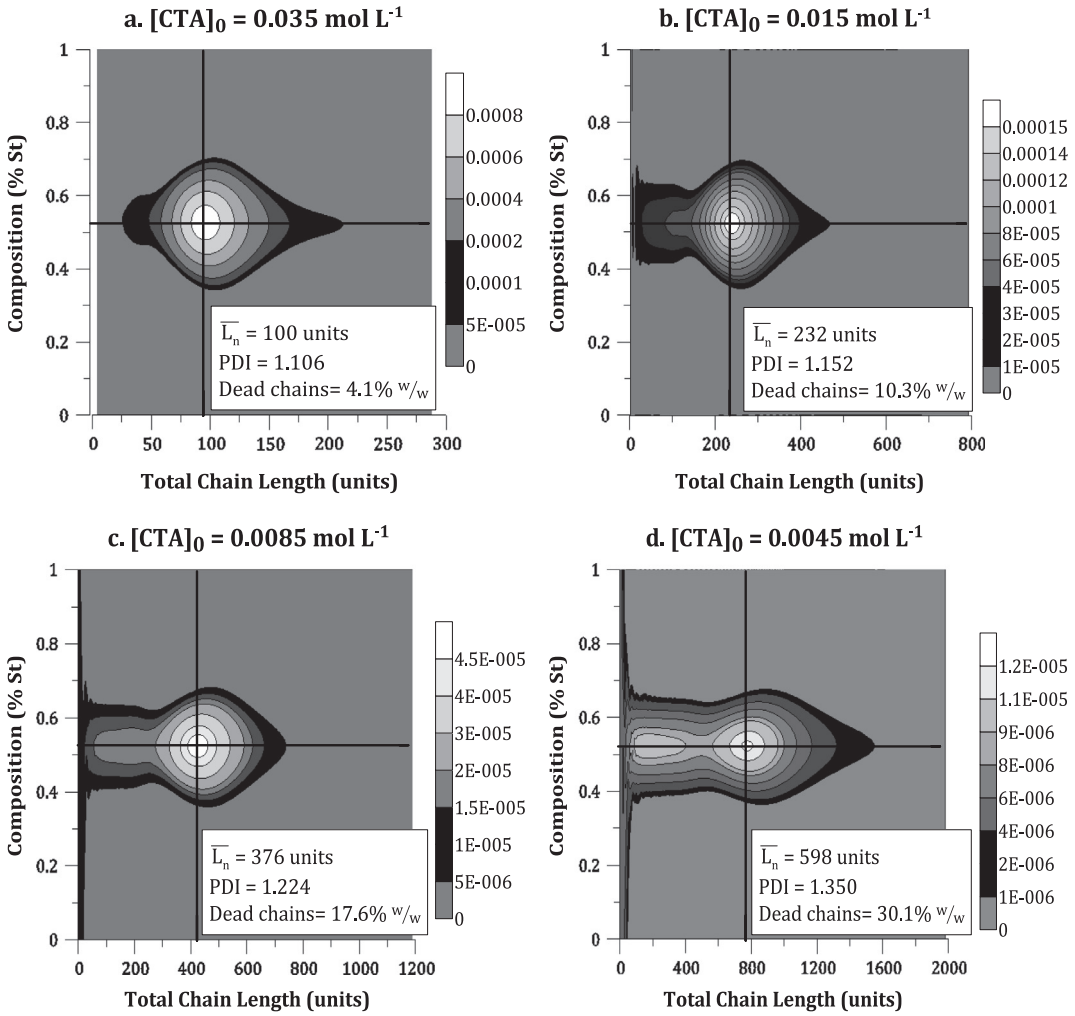

Fig. 4. MWD-CCD of copolymers with different $[CTA]_0$. Batch operation: t_{final} = 12 h, T = 60 °C, $[St]_0 = [MMA]_0$ = 4.349 mol L^{-1}, $[I]_0$ = 0.0037 mol L^{-1}.

In the following sections, other examples of the model capabilities are shown. Both batch and semibatch operation are considered.

3.2. Variation of the initial concentration of initiator

The impact of varying the initial concentration of initiator ($[I]_0$) on the copolymer properties was evaluated for a batch reactor. For this purpose, the final reaction time and the initial concentration of chain transfer agent and monomers were kept fixed, with equimolar comonomer concentrations. The results shown in this section were obtained with the mathematical model that corresponds to the SF kinetic theory. Similar results were obtained for the IRT and IRTO theories.

As can be observed in Table 2, conversion increases with the initial concentration of initiator, evidencing an increase in polymerization rate. However, the polydispersity index and fraction of dead chains are also larger, indicating a lower degree of control over the molecular structure of the polymeric material. This result is reasonable, because more initiator leads to higher concentration of free radicals, something that favors propagation and termination reactions. Therefore, the higher conversion is achieved at the expense of a higher fraction of dead polymer. Since polymer chains are dead in a higher proportion throughout the entire reaction time, this ultimately leads to material containing chains of different molecular weights and therefore higher polydispersity.

As long as the fraction of dead polymer remains low (i.e. less than 10%), the number average chain length for RAFT copolymers can be approximated by the equation:

$$\overline{L_n} \approx \frac{Conv\ ([M_A]_0 + [M_B]_0)}{[CTA]_0} \tag{30}$$

In Fig. 2 the evolution of $\overline{L_n}$ with conversion for the three $[I]_0$ under study predicted by the model are compared with the theoretical chain lengths calculated with Eq. (30). It can be observed

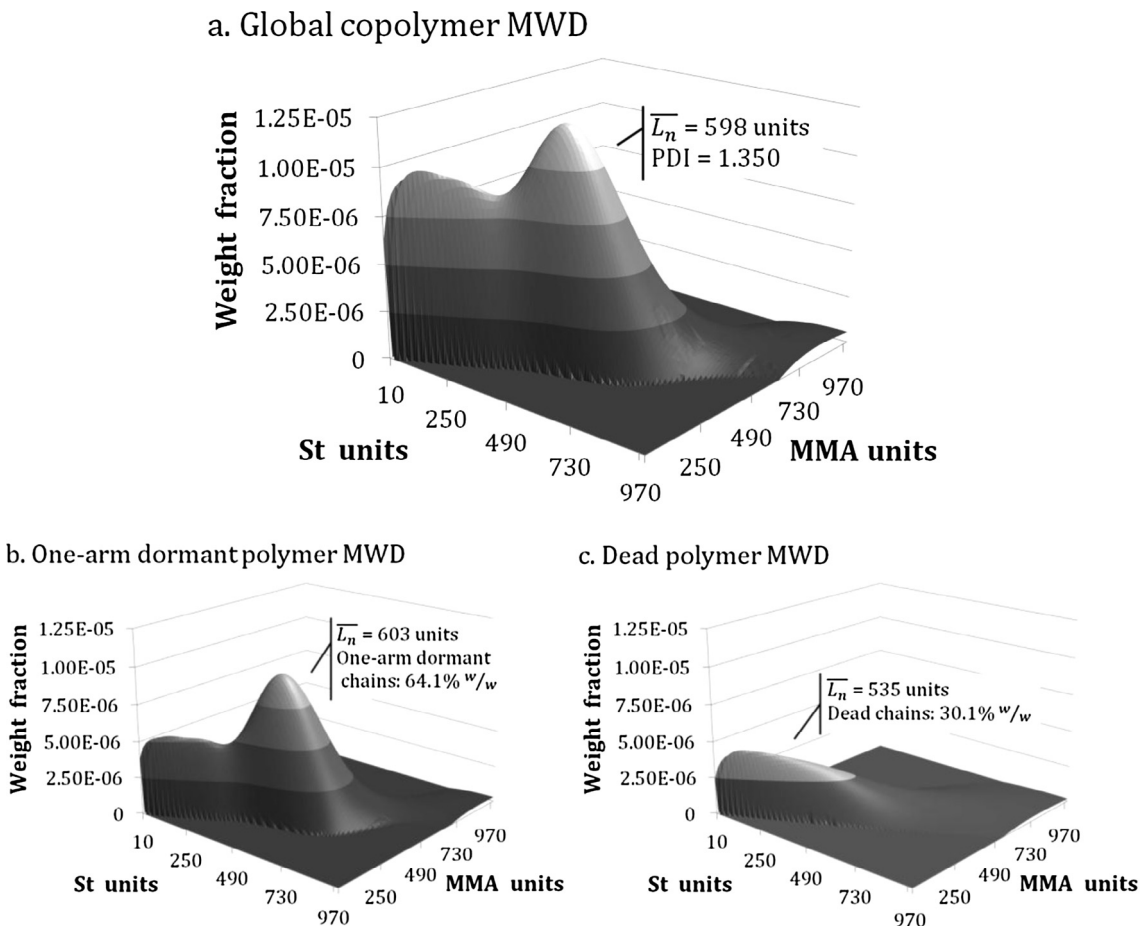

Fig. 5. MWD of (a) global copolymer, (b) one-arm dormant population, (c) dead chains population, obtained with $[CTA]_0 = 0.0045$ mol L^{-1}, $t_{final} = 12$ h, T = 60 °C, $[St]_0 = [MMA]_0 = 4.349$ mol L^{-1}, $[I]_0 = 0.0037$ mol L^{-1}, batch operation. Weight fractions of species reported in the figures.

Table 4
Polymer molecular properties for different operating policies. $t_{final} = 12$ h, T = 60 °C, $[I]_0 = 0.0037$ mol L^{-1}, $[CTA]_0 = 0.035$ mol L^{-1}, $m_{MMA,0} = 600$ g (except when it is constantly fed, in this case it is 0 g); first and last rows correspond to the semibatch operation.

$[St]_0$: $[MMA]_0$	F_{St} (g min^{-1})	F_{MMA} (g min^{-1})	Comp. (% St)	$\overline{L_n}$ (g mol^{-1})	PDI	Conv. (%)	Dead chains (w/w %)
0:100	0.867	0	38.8	95	1.115	40.1	4.03
30:70	0	0	36.7	117	1.104	49.3	4.4
50:50	0	0	52.3	100	1.106	42.2	4.1
70:30	0	0	67.1	83	1.107	34.8	3.8
100:0	0	0.833	61.7	77	1.102	32.6	3.5

that the average chain length differs the most from the theoretical value for the highest initial concentration of initiator. When the growth of polymer chains is under control, the total number of "living" chains remains approximately constant and equal to the initial concentration of chain transfer agent. This ceases to be true when a considerable number of chains takes part in termination reactions. These results are consistent with the rule of thumb that considers that the controlled radical polymerizations maintain their "livingness" provided that the fraction of dead chains is lower than 10%.

In conclusion, operating with higher initial concentration of initiator would allow producing a copolymer with a pre-specified molecular weight in a shorter time, increasing the productivity of the reaction. However, this operating policy would not be advisable if the application demanded a material with low polydispersity or if it was required to perform polymer chain extensions.

3.3. Variation of the initial concentration of chain transfer agent

Reactions with four different initial concentration of chain transfer agent ($[CTA]_0$) were simulated so as to analyze its effect on the copolymer molecular properties. Similarly to the previous study, the final reaction time and the initial concentration of initiator were kept fixed and equimolar quantities of comonomers were considered in a batch reactor. The results correspond only to the SF kinetic theory since they were similar to those obtained with IRT and IRTO theories.

Fig. 3 shows the relationship between the number-average molecular weight and conversion for the different initial concentrations of CTA. Dashed lines correspond to $\overline{L_n}$ calculated with Eq. (30) and symbols represent the average chain length computed with the complete model. It can be observed that $\overline{L_n}$ increases for a given conversion when $[CTA]_0$ is reduced. This behavior agrees with the chain length increase predicted by Eq. (30).

Note that the deviation from linearity predicted by the approximate expression increases considerably as the $[CTA]_0$ is reduced, something that is associated to the higher percentage of dead polymer chains.

Table 3 presents values of some polymer properties and conversion at the final time of the four simulated reactions. It can be seen that the higher molecular weights at lower initial concentration of CTA are achieved at the expense of increasing the termination reactions, which results in higher polydispersity indexes (less uniformity of the material) and fewer "living" chains capable of further growth or functionalization.

Figs. 4 and 5 exemplify the detailed information about the polymer structure that can be obtained from the bivariate MWD-CCD, which would not be available with just the values of PDI and average composition shown in Table 3. It can be seen in Fig. 4 that the MWD-CCD of the copolymer exhibits a "shoulder" or low peak in the region of short chain lengths, that enlarges as $[CTA]_0$ becomes smaller. This "shoulder" is due to the contribution of the dead polymer and the one-arm dormant populations. This is exemplified for the lowest $[CTA]_0$, for which this behavior is most notorious (Fig. 4d). For this case, we compare in Fig. 5 the MWD of the whole copolymer and of the populations of dead polymer chains and the one-arm dormant chains. It can be seen that the low-molecular weight peak of the global copolymer distribution corresponds to the contribution of both dead chains and one-arm dormant populations.

3.4. Variation of the comonomers feeding policy

The use of appropriate comonomer feeding policies in controlled polymerizations allows obtaining materials with distinct features due to the conformation of unique molecular architectures. In order to evaluate this effect, two operating policies were analyzed: batch operation with different initial concentration of comonomers, and semibatch operation with constant feed of St or MMA. Once again, only the results corresponding to the SF theory are presented as similar outcomes were obtained for the other kinetic theories.

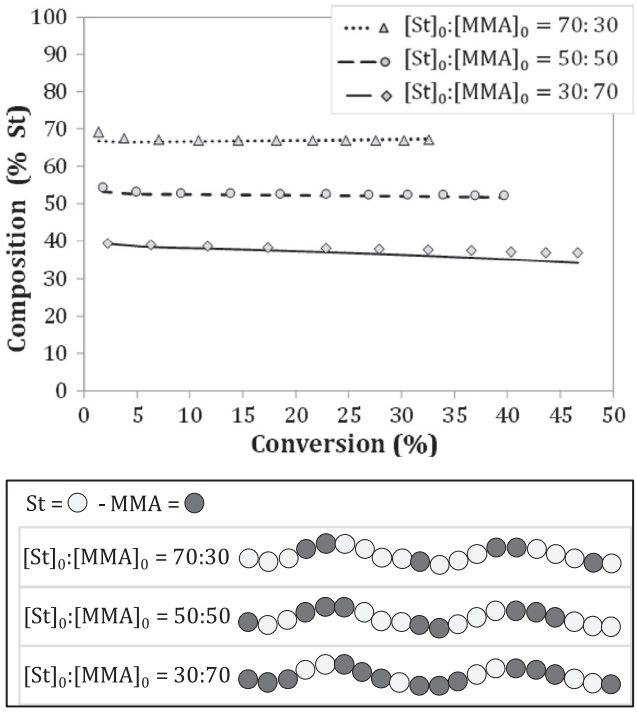

Fig. 6. Composition for different $[St]_0$:$[MMA]_0$ ratios. Lines: instantaneous composition – Symbols: cumulative composition. Batch operation: t_{final} = 12 h, T = 60 °C, $[I]_0$ = 0.0037 mol L^{-1}, $[CTA]_0$ = 0.035 mol L^{-1}.

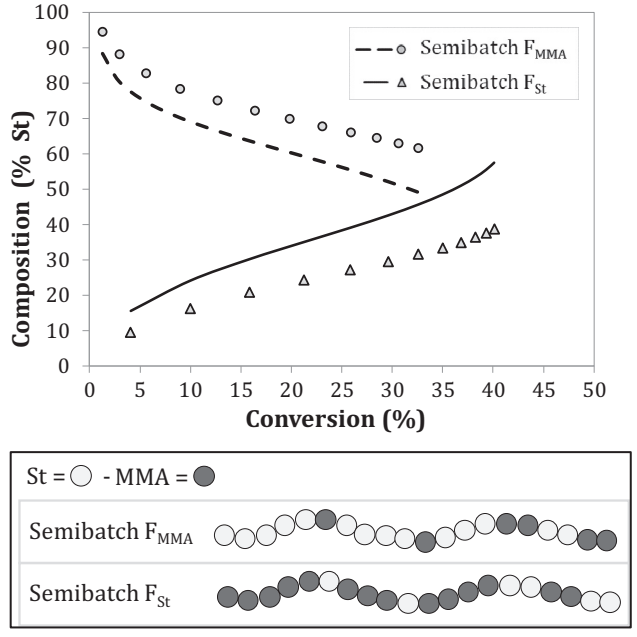

Fig. 7. Composition for constant feed of one comonomer. Lines: instantaneous composition – Symbols: cumulative composition. Semibatch operation: t_{final} = 12 h, T = 60 °C, $[I]_0$ = 0.0037 mol L^{-1}, $[CTA]_0$ = 0.035 mol L^{-1}.

In the case of batch operation, the influence of the initial ratio of comonomers on the molecular properties of the copolymers was studied. The results that are presented correspond to a reaction time of 12 h for three different ratios of St to MMA initial molar concentrations: 30:70, 50:50, and 70:30. The initial concentrations of initiator and CTA were kept fixed.

For the semibatch operation, a single total St to MMA feed molar ratio of 50:50 was considered. The operating policy consisted in feeding the entire mass of one of the comonomers at the beginning of the reaction and adding the other one at a constant rate during the entire reaction time. The initial concentrations of initiator and CTA were kept fixed and the reaction time was also 12 h.

Table 4 presents the values of the average copolymer composition, number-average molecular weights, polydispersity indexes, conversions and amount of dead chains for the five operating policies that were considered. As expected, the content of St in the copolymer increases as the initial concentration of this comonomer

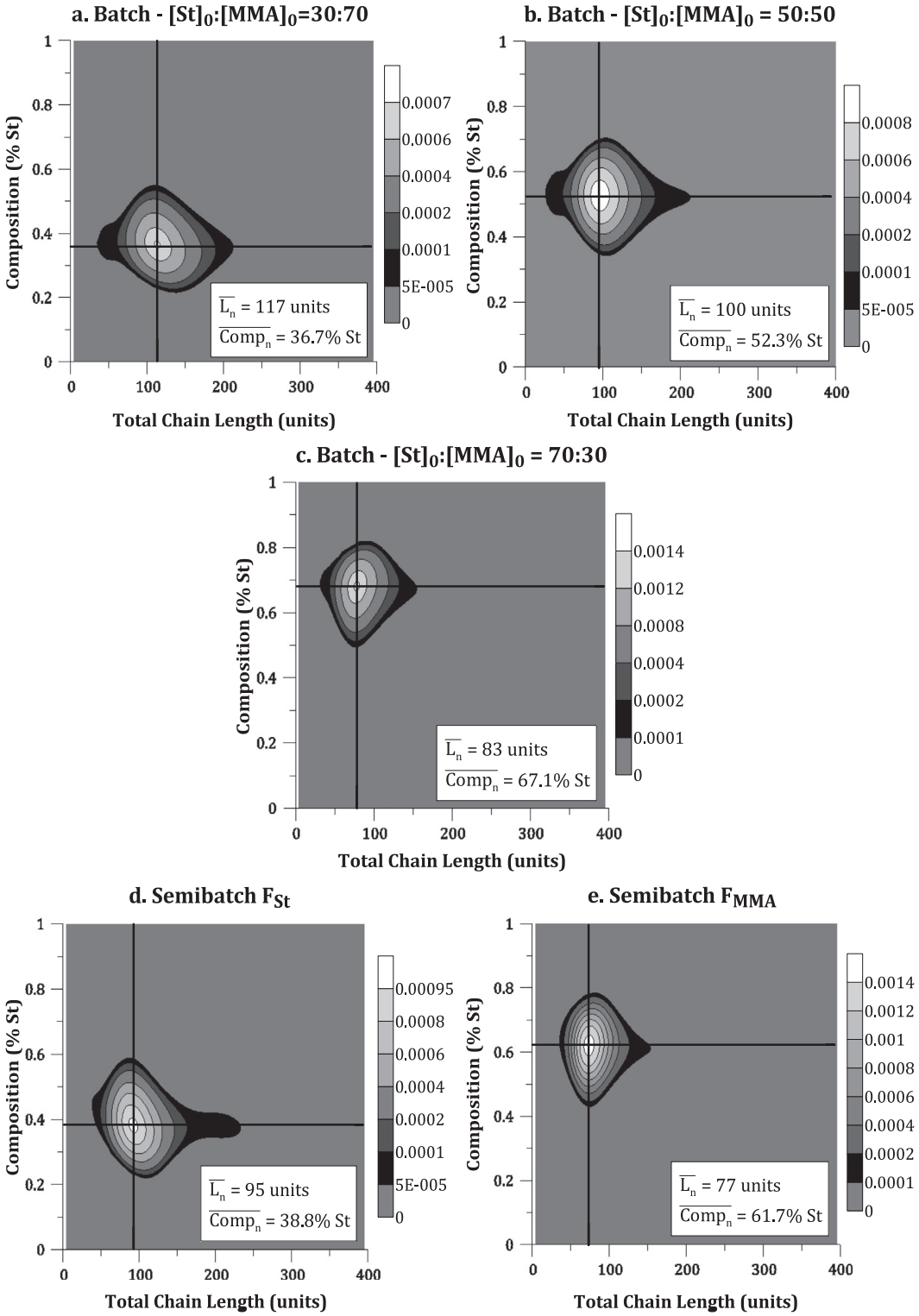

Fig. 8. MWD-CCD for different feeding policies. t_{final} = 12 h, T = 60 °C, $[I]_0$ = 0.0037 mol L^{-1}, $[CTA]_0$ = 0.035 mol L^{-1}.

is higher. In the case of the batch operation, it can be seen that the reaction rate decreases as the initial concentration of St increases, because this is the comonomer with smaller propagation kinetic constants. Consequently, molecular weights are lower for higher initial concentration of St.

Fig. 6 shows the development of cumulative and instantaneous composition with conversion for the batch operation. Taking into account that in a controlled polymerization all the chains grow at the same speed on average, the instantaneous composition allows estimating the composition along the copolymer backbone. Then, for the simulated cases, the copolymers have a uniform composition along the chains that is approximately equal to the average composition. Note that the reactivity ratios of the comonomer pair under consideration are $rx_{St} = 0.57$ and $rx_{MMA} = 0.41$. In consequence, in a spontaneous batch polymerization the copolymer will take an approximately alternating structure. The copolymer composition values reported in Table 4 and the copolymer composition profiles shown in Fig. 6 are the expected ones given the reactivity ratios of the comonomers. On the other hand, a spontaneous gradient copolymer would result if one of the reactivity ratios were greater than one [56]. The model presented in this work is also able to capture this behavior. Having both reactivity ratios less than unity makes it more difficult to synthesize gradient copolymers because this structure is not obtained spontaneously. In this case, appropriate feeding policies are required to achieve the gradient profile along the chain. Therefore, models able to predict the copolymer composition are of great help to determine the operating conditions for each targeted structure [28,57,58].

A considerably different structure can be obtained in the semibatch operation. The evolution of cumulative and instantaneous composition with conversion for this case is shown in Fig. 7. In the figures that follow, the operating policy consisting in feeding either St or MMA at constant rate (first and last rows in Table 4) is referred to as "Semibatch F_{St}" or "Semibatch F_{MMA}", respectively. When the whole mass of MMA is fed at the beginning of the reaction, the final copolymer composition is similar to that obtained in batch operation for $[St]_0$:$[MMA]_0$ = 30:70. Similarly, when St is the monomer fed entirely at the start, the final copolymer composition resembles that obtained in batch operation for $[St]_0$:$[MMA]_0$ = 70:30. However, in both cases the achieved structure is very different since the constant feed of one of the monomers allows obtaining a more gradient-like structure, as illustrated in the schematic drawing in Fig. 7.

Fig. 8 shows the MWD-CCD of the produced copolymers. As previously explained, these distributions can offer extra information about the molecular structure of polymer chains. It can be seen that distributions are narrow in both dimensions and have no secondary peaks, which indicates that the obtained material is uniform.

It can also be noted that when the copolymer has an approximately equal content of both comonomers (Fig. 8b), there is symmetry around the average composition axes and around the number average chain length axis, as discussed before. However, this symmetry is not maintained when one of the comonomers is more abundant than the other in the copolymer. In these cases, Fig. 8a and c, longer chains (see vertical slices) are richer in the comonomer with higher composition than shorter chains. The MWD-CCD obtained with the semibatch operation are similar to those of the batch operation that yield copolymers with similar average composition.

The model presented in this work could be easily extended to include the prediction of the sequence length distribution [54]. However, such detailed study on the copolymer structure is out of the scope of this article.

4. Conclusions

In this work, we presented a successful model for the RAFT copolymerization that includes the bivariate MWD-CCD of the copolymer. The complex nature of the intermediate adduct was taken into account, something that required considering a 4-dimensional species. As discussed above, the model may provide valuable information on the influence of operating conditions on the quality of the product and the productivity of the process. Finally, the bivariate MWD-CCD was shown to be very useful in providing detailed information on the molecular structure of the copolymer that would be very difficult to obtain experimentally. This would have a practical application for establishing operating conditions suitable for obtaining the structure required by particular end uses.

Acknowledgements

The authors acknowledge the financial support of CONICET (Consejo Nacional de Investigaciones Científicas y Técnicas, Argentina), and UNS (Universidad Nacional del Sur).

Appendix A

A.1. Reaction rate terms, r_X, in balance equations

The final expressions for the reaction terms that must be used in the mass balances of low molecular weight species as well as in the moment and pgf balances of polymeric species, represented generically by Eq. (14), are:

Initiator:

$$r_I = -k_d[I] \tag{A.1}$$

Chain transfer agent (TR_0):

$$r_{TR_0} = -k^0_{a,A}[TR_0]\lambda^A_{0,0} - k^0_{a,B}[TR_0]\lambda^B_{0,0} + \left(\frac{1}{2}\right) k^0_{f,A}\,\omega^A_{0,0} + \left(\frac{1}{2}\right)k^0_{f,B}\,\omega^B_{0,0} \tag{A.2}$$

Monomer j (j = A: styrene, j = B: methyl methacrylate):

$$r_{M_j} = -(2fk_d[I] + k^0_{f,A}\,\omega^A_{0,0} + k^0_{f,B}\,\omega^B_{0,0})\left(\frac{[M_j]}{[M_j]+[M_i]}\right) - 3k_{th}[M_j]^3\delta_{j,A} - (k_{p,Aj} + k_{trm,Aj})[M_j]\lambda^A_{0,0} - (k_{p,Bj} + k_{trm,Bj})[M_j]\lambda^B_{0,0} \tag{A.3}$$

Radicals with a final unit of monomer A, *n units of* M_A *and m units of* M_B:

$$\begin{aligned} r_{R^A_{n,m}} = {} & \left\{ \begin{matrix} (2fk_d[I] + k^0_{f,A}\,\omega^A_{0,0} + k^0_{f,B}\,\omega^B_{0,0})\left(\frac{[M_A]}{[M_A]+[M_B]}\right) \\ +(k_{trm,AA}\lambda^A_{0,0} + k_{trm,BA}\lambda^B_{0,0})[M_A] \end{matrix} \right\}\delta_{n,1}\delta_{m,0} \\ & + k_{th}[M_A]^3(\delta_{n,1}\delta_{m,0} + \delta_{n,2}\delta_{m,0}) + \left(\tfrac{1}{2}\right)k^0_{f,A}\,[R^A_{n,m}TR_0] \\ & + [M_A](1 - \delta_{n,1}\delta_{m,0} - \delta_{n,0})(k_{p,AA}[R^A_{n-1,m}] + k_{p,BA}[R^B_{n-1,m}]) \\ & - \left\{ \begin{matrix} (k_{p,AA} + k_{trm,AA})[M_A] + (k_{p,AB} + k_{trm,AB})[M_B] \\ +(k_{tc,AA} + k_{td,AA})\lambda^A_{0,0} + (k_{tc,AB} + k_{td,AB})\lambda^B_{0,0} \end{matrix} \right\}[R^A_{n,m}] \\ & + \left(\tfrac{1}{2}\right)k_{f,A}\,(d\gamma^{AA}_{n,m} + d\gamma^{AB}_{n,m}) - \left\{k_{a,A}(\omega^A_{0,0} + \omega^B_{0,0}) + k^0_{a,A}[TR_0]\right\}[R^A_{n,m}] \\ & - k_{c,A}\left(\begin{matrix} \gamma^{AA}_{0,0} + \gamma^{AB}_{0,0} + \gamma^{BB}_{0,0} \\ +\omega^A_{0,0} + \omega^B_{0,0} \end{matrix} \right)[R^A_{n,m}] \left\{ \begin{matrix} \delta_{theory,IRT} + \\ \left(\begin{matrix} \delta_{n,1}\delta_{m,1} + \delta_{n,1}\delta_{m,0} \\ +\delta_{n,2}\delta_{m,0} \end{matrix} \right)\delta_{theory,IRTO} \end{matrix} \right\} \end{aligned} \tag{A.4}$$

Radicals with a final unit of monomer B, *n units of* M_A *and m units of* M_B*:*

$$r_{R^B_{n,m}} = \left\{ \begin{array}{l} (2fk_d[I] + (\tfrac{1}{2})k^0_{f,B}\,\omega^B_{0,0} + (\tfrac{1}{2})k^0_{f,A}\,\omega^A_{0,0})\left(\frac{[M_B]}{[M_A]+[M_B]}\right) \\ +(k_{trm,BB}\lambda^B_{0,0} + k_{trm,AB}\lambda^A_{0,0})[M_B] \end{array} \right\}\delta_{n,0}\delta_{m,1}$$
$$+[M_B](1-\delta_{n,0}\delta_{m,1}-\delta_{m,0})(k_{p,AB}[R^A_{n,m-1}] + k_{p,BB}[R^B_{n,m-2}])$$
$$-\left\{ \begin{array}{l} (k_{p,BB}+k_{trm,BB})[M_B] + (k_{p,BA}+k_{trm,BA})[M_A] \\ +(k_{tc,BB}+k_{td,BB})\lambda^B_{0,0} + (k_{tc,AB}+k_{td,AB})\lambda^A_{0,0} \end{array} \right\}[R^B_{n,m}] + (\tfrac{1}{2})k^0_{f,B}\,[R^B_{n,m}TR_0]$$
$$+(\tfrac{1}{2})k_{f,B}\,(d\gamma^{BB}_{n,m} + d\gamma^{BA}_{n,m}) - \left\{k_{a,B}(\omega^B_{0,0}+\omega^A_{0,0}) + k^0_{a,B}[TR_0]\right\}[R^B_{n,m}]$$
$$-k_{c,B}\left(\begin{array}{l} \gamma^{AA}_{0,0} + \gamma^{AB}_{0,0} + \gamma^{BB}_{0,0} \\ +\omega^A_{0,0} + \omega^B_{0,0} \end{array} \right)[R^B_{n,m}]\left\{ \begin{array}{l} \delta_{theory,IRT} + \\ (\delta_{n,1}\delta_{m,1} + \delta_{n,0}\delta_{m,1}) \\ +\delta_{n,0}\delta_{m,2} \end{array} \right\}\delta_{theory,IRTO} \tag{A.5}$$

One-arm dormant copolymer with a final unit of monomer j (j = A, B*), n units of* M_A *and m units of* M_B*:*

$$r_{TR^j_{n,m}} = \left(\frac{1}{2}\right)k^0_{f,j}[R^j_{n,m}TR_0] + \left(\frac{1}{2}\right)k_{f,j}\,d\gamma^{j,j}_{n,m} + \left(\frac{1}{2}\right)k_{f,i}\,d\gamma^{j,i}_{n,m} - (k_{a,i}\,\lambda^i_{0,0} + k_{a,j}\,\lambda^j_{0,0})[TR^j_{n,m}] \tag{A.6}$$

Two-arm adduct radicals in pre-equilibrium (one branch with 0 units in length) with a final unit of monomer i (i = A, B*), n units of* M_A *and m units of* M_B*:*

$$r_{R^i_{n,m}TR_0} = k^0_{a,i}\,[TR_0]\,[R^i_{n,m}] - k^0_{f,i}\,[R^i_{n,m}TR_0] - \left(\begin{array}{l} k_{c,A}\,(\lambda^A_{0,0}\delta_{theory,IRT} + ([R^A_{1,1}] + [R^A_{1,0}] + [R^A_{2,0}])\delta_{theory,IRTO}) + \\ k_{c,B}\,(\lambda^B_{0,0}\delta_{theory,IRT} + ([R^B_{1,1}] + [R^B_{0,1}] + [R^B_{0,2}])\delta_{theory,IRTO}) \end{array} \right)[R^i_{n,m}TR_0] \tag{A.7}$$

Two-arm adduct radicals in the main equilibrium: first branch with a final unit of monomer i, n units of M_A *and m units of* M_B*; second branch with a final unit of monomer j, g units of* M_A *and h units of* M_B *(i, j =* A, B*):*

$$r_{R^i_{n,m}TR^j_{g,h}} = k_{a,i}\,[R^i_{n,m}][TR^j_{g,h}] + k_{a,j}\,[TR^i_{n,m}][R^j_{g,h}] - \left(\frac{1}{2}\right)k_{f,i}\,[R^i_{n,m}TR^j_{g,h}] - \left(\frac{1}{2}\right)k_{f,j}\,[R^i_{n,m}TR^j_{g,h}] - \left(\begin{array}{l} k_{c,A}\left(\lambda^A_{0,0}\delta_{theory,IRT} + ([R^A_{1,1}] + [R^A_{1,0}] + [R^A_{2,0}])\delta_{theory,IRTO}\right) + \\ k_{c,B}\left(\lambda^B_{0,0}\delta_{theory,IRT} + ([R^B_{1,1}] + [R^B_{0,1}] + [R^B_{0,2}])\delta_{theory,IRTO}\right) \end{array} \right)[R^i_{n,m}TR^j_{g,h}] \tag{A.8}$$

Two-arm adduct radicals with a final unit of monomer i in the first branch and a final unit of monomer j (i, j = A, B*) in the other branch, considering the total number of units of each comonomer (n units of* M_A *and m units of* M_B*, adding the units in both arms):*

$$r_{(R^iTR^j)_{n,m}} = k_{a,i}\sum_{g=0}^{n-1}\sum_{h=0}^{m-1}[R^i_{n-g,m-h}][TR^j_{g,h}] + k_{a,j}\sum_{g=0}^{n-1}\sum_{h=0}^{m-1}[R^j_{n-g,m-h}][TR^i_{g,h}] - \left(\frac{1}{2}\right)(k_{f,i}+k_{f,j})\,[(R^iTR^j)_{n,m}] - \left(\begin{array}{l} k_{c,A}\,(\lambda^A_{0,0}\delta_{theory,IRT} + ([R^A_{1,1}] + [R^A_{1,0}] + [R^A_{2,0}])\delta_{theory,IRTO}) + \\ k_{c,B}\,(\lambda^B_{0,0}\delta_{theory,IRT} + ([R^B_{1,1}] + [R^B_{0,1}] + [R^B_{0,2}])\delta_{theory,IRTO}) \end{array} \right)\left[(R^iTR^j)_{n,m}\right] \tag{A.9}$$

Dead copolymer radicals with n units of M_A *and m units of* M_B*:*

$$r_{P_{n,m}} = (k_{trm,AA}[M_A] + k_{trm,AB}[M_B] + k_{td,AA}\lambda^A_{0,0} + k_{td,AB}\lambda^B_{0,0})[R^A_{n,m}] + (k_{trm,BA}[M_A] + k_{trm,BB}[M_B] + k_{td,BA}\lambda^A_{0,0} + k_{td,BB}\lambda^B_{0,0})[R^B_{n,m}] + k_{tc,AB}\sum_{l=0}^{n-l}\sum_{r=0}^{m-r}[R^A_{n-l,m-r}][R^B_{l,r}] + (\tfrac{1}{2})k_{tc,AA}\sum_{l=0}^{n-l}\sum_{r=0}^{m-r}[R^A_{n-l,m-r}][R^A_{l,r}] + (\tfrac{1}{2})k_{tc,BB}\sum_{l=0}^{n-l}\sum_{r=0}^{m-r}[R^B_{n-l,m-r}][R^B_{l,r}]$$
$$+k_{c,A}\left\{ \begin{array}{l} \left(\sum_{l=2}^{n-2}\sum_{r=0}^{m}[R^A_{n-l,m-r}][(R^ATR^A)_{l,r}]\right) + \\ \left(\sum_{l=1}^{n-1}\sum_{r=1}^{m-1}[R^A_{n-l,m-r}][(R^ATR^B)_{l,r}]\right) + \\ \left(\sum_{l=0}^{n}\sum_{r=2}^{m-2}[R^A_{n-l,m-r}][(R^BTR^B)_{l,r}]\right) + \\ \left(\sum_{l=1}^{n-1}\sum_{r=0}^{m}[R^A_{n-l,m-r}][R^A_{l,r}TR_0]\right) + \\ \left(\sum_{l=0}^{n}\sum_{r=1}^{m-1}[R^A_{n-l,m-r}][R^B_{l,r}TR_0]\right) \end{array} \right\}\left(\begin{array}{l} \delta_{theory,IRT} + \\ (\delta_{n,1}\delta_{m,1} + \\ \delta_{n,1}\delta_{m,0} + \\ \delta_{n,2}\delta_{m,0} \end{array} \right)\delta_{theory,IRTO}$$
$$+k_{c,B}\left\{ \begin{array}{l} \left(\sum_{l=2}^{n-2}\sum_{r=0}^{m}[R^B_{n-l,m-r}][(R^ATR^A)_{l,r}]\right) + \\ \left(\sum_{l=1}^{n-1}\sum_{r=1}^{m-1}[R^B_{n-l,m-r}][(R^ATR^B)_{l,r}]\right) + \\ \left(\sum_{l=0}^{n}\sum_{r=2}^{m-2}[R^B_{n-l,m-r}][(R^BTR^B)_{l,r}]\right) + \\ \left(\sum_{l=1}^{n-1}\sum_{r=0}^{m}[R^B_{n-l,m-r}][R^A_{l,r}TR_0]\right) + \\ \left(\sum_{l=0}^{n}\sum_{r=1}^{m-1}[R^B_{n-l,m-r}][R^B_{l,r}TR_0]\right) \end{array} \right\}\left(\begin{array}{l} \delta_{theory,IRT} + \\ (\delta_{n,1}\delta_{m,1} + \\ \delta_{n,0}\delta_{m,1} + \\ \delta_{n,0}\delta_{m,2} \end{array} \right)\delta_{theory,IRTO} \tag{A.10}$$

Please note that the summations that appear in the original reaction terms presented in this Appendix were replaced by the corresponding moment definitions in Section 2.4.1. The same was done in the reaction terms in the mass balances of macromolecular species prior to their transformation using the moment and pgf techniques.

Reaction terms in moment balances

The reaction rate expressions that must be used in the moment balances of the polymeric species may be deduced from Eqs. (A.1)–(A.10) by applying the corresponding moment definitions. This process results in the following equation for the moment reaction rate:

Partial moment of order 0,0 of two-arm adduct radicals in the main equilibrium: first branch with a final unit of monomer i, n units of M_A *and m units of* M_B*; second branch with a final unit of monomer j, g units of* M_A *and h units of* M_B *(i, j =* A, B*):*

$$r_{d\gamma^{i,j}_{n,m}} = k_{a,i}\mu^j_{0,0}\,[R^i_{n,m}] + k_{a,j}\lambda^j_{0,0}\,[TR^i_{n,m}] - (\tfrac{1}{2})k_{f,i}d\gamma^{i,j}_{n,m} - (\tfrac{1}{2})k_{f,j}d\gamma^{i,j}_{n,m} - \left(\begin{array}{l} k_{c,A}\,(\lambda^A_{0,0}\delta_{theory,IRT} + ([R^A_{1,1}] + [R^A_{1,0}] + [R^A_{2,0}])\delta_{theory,IRTO}) + \\ k_{c,B}\,(\lambda^B_{0,0}\delta_{theory,IRT} + ([R^B_{1,1}] + [R^B_{0,1}] + [R^B_{0,2}])\delta_{theory,IRTO}) \end{array} \right)d\gamma^{i,j}_{n,m} \tag{A.11}$$

It is clear from the kinetic scheme presented in Section 2.3 that in the IRTO model the mass balances of short radicals (up to 2 units in length, in all possible combinations, that is $n + m = 2$) must be posed according to Eqs. (A.4) and (A.5). As the concentrations of other short species appear in those equations, it is also necessary to pose mass balances for them, that is: for oligomeric one-arm

dormant radicals (Eq. (A.6)), two-arms adduct radicals in pre-equilibrium (Eq. (A.7)) and partial moment of the two-arms adduct radicals in the main equilibrium (Eq. (A.11)). For the other theories, these mass balances are not required since they are replaced by the corresponding moment and pgf equations.

Moment of order a,b (a,b = 0,0; 0,1; 0,2; 1,1; 1,0; 2,0) of active radicals with a final unit of monomer A, *n units of* M_A *and m units of* M_B:

$$
\begin{aligned}
r_{\lambda^{A}_{a,b}} &= \left\{ \begin{array}{l} \left\{ 2fk_d[I] + \left(\tfrac{1}{2}\right) \begin{pmatrix} k^0_{f,A}\,\omega^A_{0,0} \\ +k^0_{f,B}\,\omega^B_{0,0} \end{pmatrix} \right\} \left(\frac{[M_A]}{[M_A]+[M_B]}\right) \\ +\left(k_{trm,AA}\lambda^A_{0,0} + k_{trm,BA}\lambda^B_{0,0}\right)[M_A] \end{array} \right\} 1^a 0^b \\
&+ k_{th}[M_A]^3 (1^a 0^b + 2^a 0^b) + \left(\tfrac{1}{2}\right) k^0_{f,A}\,\omega^A_{a,b} \\
&+ k_{p,AA}[M_A] \sum_{h=0}^{a} \binom{a}{h} \lambda^A_{a-h,b} + k_{p,AB}[M_A] \sum_{h=0}^{a} \binom{a}{h} \lambda^B_{a-h,b} \\
&- \left\{ \begin{array}{l} (k_{p,AA} + k_{trm,AA})[M_A] + (k_{p,AB} + k_{trm,AB})[M_B] + \\ +(k_{tc,AA} + k_{td,AA})\lambda^A_{0,0} + (k_{tc,AB} + k_{td,AB})\lambda^B_{0,0} \end{array} \right\} \lambda^A_{a,b} \\
&+ \left(\tfrac{1}{2}\right) k_{f,A}\,(\gamma^{AA}_{a,b} + \gamma^{AB}_{a,b}) - \left\{ k_{a,A}(\omega^A_{0,0} + \omega^B_{0,0}) + k^0_{a,A}[TR_0] \right\} \lambda^A_{a,b} \\
&- k_{c,A} \begin{pmatrix} \gamma^{AA}_{0,0} + \gamma^{AB}_{0,0} + \gamma^{BB}_{0,0} \\ +\omega^A_{0,0} + \omega^B_{0,0} \end{pmatrix} \left\{ \begin{array}{l} \lambda^A_{a,b}\delta_{theory,IRT} + \\ \left(\begin{array}{l} 1^a 1^b [R^A_{1,1}] + 1^a 0^b [R^A_{1,0}] \\ +2^a 0^b [R^A_{2,0}] \end{array} \right) \delta_{theory,IRTO} \end{array} \right\}
\end{aligned}
\tag{A.12}
$$

Moment of order a,b (a,b = 0,0; 0,1; 0,2; 1,1; 1,0; 2,0) of active radicals with a final unit of monomer B, *n units of* M_A *and m units of* M_B:

$$
\begin{aligned}
r_{\lambda^{B}_{a,b}} &= \left\{ \begin{array}{l} \left\{ 2fk_d[I] + \left(\tfrac{1}{2}\right) \begin{pmatrix} k^0_{f,A}\,\omega^A_{0,0} \\ +k^0_{f,B}\,\omega^B_{0,0} \end{pmatrix} \right\} \left(\frac{[M_B]}{[M_A]+[M_B]}\right) \\ +\left(k_{trm,Aj}\lambda^A_{0,0} + k_{trm,Bj}\lambda^B_{0,0}\right)[M_j] \end{array} \right\} 0^a 1^b \\
&+ k_{p,BA}[M_B] \sum_{g=0}^{b} \binom{b}{g} \lambda^A_{a,b-g} + k_{p,BB}[M_B] \sum_{g=0}^{b} \binom{b}{g} \lambda^B_{a,b-g} \\
&- \left\{ \begin{array}{l} (k_{p,BB} + k_{trm,BB})[M_B] + (k_{p,BA} + k_{trm,BA})[M_A] + \\ +(k_{tc,BB} + k_{td,BB})\lambda^B_{0,0} + (k_{tc,BA} + k_{td,BA})\lambda^A_{0,0} \end{array} \right\} \lambda^B_{a,b} + \left(\tfrac{1}{2}\right) k^0_{f,2}\,\omega^B_{a,b} \\
&+ \left(\tfrac{1}{2}\right) k_{f,B}\,(\gamma^{BB}_{a,b} + \gamma^{BA}_{a,b}) - \left\{ k_{a,B}(\omega^B_{0,0} + \omega^A_{0,0}) + k^0_{a,B}[TR_0] \right\} \lambda^B_{a,b} \\
&- k_{c,B} \begin{pmatrix} \gamma^{AA}_{0,0} + \gamma^{AB}_{0,0} + \gamma^{BB}_{0,0} \\ +\omega^A_{0,0} + \omega^B_{0,0} \end{pmatrix} \left\{ \begin{array}{l} \lambda^B_{a,b}\delta_{theory,IRT} + \\ \left(\begin{array}{l} 1^a 1^b [R^B_{1,1}] + 0^a 1^b [R^B_{0,1}] \\ +0^a 2^b [R^B_{0,2}] \end{array} \right) \delta_{theory,IRTO} \end{array} \right\}
\end{aligned}
\tag{A.13}
$$

Moment of order a,b (a,b = 0,0; 0,1; 0,2; 1,1; 1,0; 2,0) of one-arm dormant radicals with a final unit of monomer j (j = A, B*), n units of* M_A *and m units of* M_B:

$$
\begin{aligned}
r_{\mu^{j}_{a,b}} &= \left(\frac{1}{2}\right)(k^0_{f,j}\,\omega^j_{a,b} + k_{f,j}\,\gamma^{j,j}_{a,b} + k_{f,i}\,\gamma^{j,i}_{a,b}) - (k_{a,i}\,\lambda^i_{0,0} \\
&\quad + k_{a,j}\,\lambda^j_{0,0})\mu^j_{a,b}
\end{aligned}
\tag{A.14}
$$

Moment of order a,b (a,b = 0,0; 0,1; 0,2; 1,1; 1,0; 2,0) of two-arm adduct radicals in pre-equilibrium (one branch with 0 units in length) with a final unit of monomer j (j = A, B*), n units of* M_A *and m units of* M_B:

$$
\begin{aligned}
r_{\omega^{j}_{a,b}} &= k^0_{a,j}\,[TR_0]\,\lambda^j_{a,b} - k^0_{f,j}\,\omega^j_{a,b} \\
&- \begin{pmatrix} k_{c,A}\,(\lambda^A_{0,0}\delta_{theory,IRT} + ([R^A_{1,1}] + [R^A_{1,0}] + [R^A_{2,0}])\delta_{theory,IRTO}) + \\ k_{c,B}\,(\lambda^B_{0,0}\delta_{theory,IRT} + ([R^B_{1,1}] + [R^B_{0,1}] + [R^B_{0,2}])\delta_{theory,IRTO}) \end{pmatrix} \omega^j_{a,b}
\end{aligned}
\tag{A.15}
$$

Moment of order a,b (a,b = 0,0; 0,1; 0,2; 1,1; 1,0; 2,0) of the partial moment of order 0,0 of two-arm adduct radicals with a final unit of monomer i of the first branch and a final unit of monomer j in the other branch (i, j = A, B*):*

$$
\begin{aligned}
r_{\gamma^{i,j}_{a,b}} &= k_{a,i}\,\mu^j_{0,0}\,\lambda^i_{a,b} + k_{a,j}\,\lambda^j_{0,0}\,\mu^i_{a,b} - \left(\tfrac{1}{2}\right) k_{f,i}\,\gamma^{i,j}_{a,b} - \left(\tfrac{1}{2}\right) k_{f,j}\,\gamma^{i,j}_{a,b} \\
&- \begin{pmatrix} k_{c,A}\,(\lambda^A_{0,0}\delta_{theory,IRT} + ([R^A_{1,1}] + [R^A_{1,0}] + [R^A_{2,0}])\delta_{theory,IRTO}) + \\ k_{c,B}\,(\lambda^B_{0,0}\delta_{theory,IRT} + ([R^B_{1,1}] + [R^B_{0,1}] + [R^B_{0,2}])\delta_{theory,IRTO}) \end{pmatrix} \gamma^{i,j}_{a,b}
\end{aligned}
\tag{A.16}
$$

Moment of order a,b (a,b = 0,0; 0,1; 0,2; 1,1; 1,0; 2,0) of the two-arm adduct radicals with a final unit of monomer i in the first branch and a final unit of monomer j (i, j = A, B*) in the other branch, considering the total number of units of each comonomer (n units of* M_A *and m units of* M_B*, adding the units in both arms):*

$$
\begin{aligned}
r_{\theta^{i,j}_{a,b}} &= k_{a,i} \sum_{j=0}^{a}\sum_{g=0}^{b} \binom{a}{j}\binom{b}{g} \mu^j_{a-j,b-g}\,\lambda^i_{a,b} + k_{a,j} \sum_{j=0}^{a}\sum_{g=0}^{b} \binom{a}{j}\binom{b}{g} \lambda^j_{a-j,b-g}\,\mu^i_{a,b} \\
&- \left\{ \begin{array}{l} \left(\tfrac{1}{2}\right)(k_{f,i} + k_{f,j}) + \\ k_{c,A}\,(\lambda^A_{0,0}\delta_{theory,IRT} + ([R^A_{1,1}] + [R^A_{1,0}] + [R^A_{2,0}])\delta_{theory,IRTO}) + \\ k_{c,B}\,(\lambda^B_{0,0}\delta_{theory,IRT} + ([R^B_{1,1}] + [R^B_{0,1}] + [R^B_{0,2}])\delta_{theory,IRTO}) \end{array} \right\} \theta^{i,j}_{a,b}
\end{aligned}
\tag{A.17}
$$

Moment of order a,b (a,b = 0,0; 0,1; 0,2; 1,1; 1,0; 2,0) of dead polymer radicals with n units of M_A *and m units of* M_B:

$$
\begin{aligned}
r_{\varepsilon_{a,b}} &= (k_{trm,AA}[M_A] + k_{trm,AB}[M_B] + k_{td,AA}\lambda^A_{0,0} + k_{td,AB}\lambda^B_{0,0})\lambda^A_{a,b} \\
&+ \left(k_{trm,BA}[M_A] + k_{trm,BB}[M_B] + k_{td,BA}\lambda^A_{0,0} + k_{td,BB}\lambda^B_{0,0}\right)\lambda^B_{a,b} \\
&+ k_{tc,AB} \sum_{j=0}^{a}\sum_{g=0}^{b} \binom{a}{j}\binom{b}{g} \lambda^A_{a-j,b-g}\,\lambda^B_{j,g} + \left(\tfrac{1}{2}\right) k_{tc,AA} \sum_{j=0}^{a}\sum_{g=0}^{b} \binom{a}{j}\binom{b}{g} \lambda^A_{a-j,b-g}\,\lambda^A_{j,g} \\
&+ \left(\tfrac{1}{2}\right) k_{tc,BB} \sum_{j=0}^{a}\sum_{g=0}^{b} \binom{a}{j}\binom{b}{g} \lambda^B_{a-j,b-g}\,\lambda^B_{j,g} \\
&+ k_{c,A} \sum_{j=0}^{a}\sum_{g=0}^{b} \binom{a}{j}\binom{b}{g} \begin{pmatrix} \theta^{AA}_{a-j,b-g} + \theta^{AB}_{a-j,b-g} \\ +\theta^{BB}_{a-j,b-g} \\ +\omega^A_{a-j,b-g} + \omega^B_{a-j,b-g} \end{pmatrix} \left\{ \begin{array}{l} \lambda^A_{j,g}\delta_{theory,IRT} + \\ \left(\begin{array}{l} 1^j 1^g [R^A_{1,1}] + \\ 1^j 0^g [R^A_{1,0}] + \\ 2^j 0^g [R^A_{2,0}] \end{array} \right) \delta_{theory,IRTO} \end{array} \right\} \\
&+ k_{c,B} \sum_{j=0}^{a}\sum_{g=0}^{b} \binom{a}{j}\binom{b}{g} \begin{pmatrix} \theta^{AA}_{a-j,b-g} + \theta^{AB}_{a-j,b-g} \\ +\theta^{BB}_{a-j,b-g} \\ +\omega^A_{a-j,b-g} + \omega^B_{a-j,b-g} \end{pmatrix} \left\{ \begin{array}{l} \lambda^B_{j,g}\delta_{theory,IRT} + \\ \left(\begin{array}{l} 1^j 1^g [R^B_{1,1}] + \\ 0^j 1^g [R^B_{0,1}] + \\ 0^j 2^g [R^B_{0,2}] \end{array} \right) \delta_{theory,IRTO} \end{array} \right\}
\end{aligned}
\tag{A.18}
$$

The following expressions correspond to the reaction terms to be used in the pgf balance equations. As previously explained, the order 0,0 pgf transform balances can be used to compute the bivariate molecular weight distribution reported in number fraction (MWD_n). The molecular weight distribution reported in weight fraction (MWD_w) can be calculated from it by algebraic manipulation. The methodology for obtaining the MWD_w may be found elsewhere [51,54].

Pgf of order 0,0 of active radicals with a final unit of monomer A:

$$r_{\lambda^{A}_{0,0}\sigma^{A}_{0,0}}(z,w)=\left\{\begin{array}{l}\left\{2fk_{d}[I]+\left(\frac{1}{2}\right)\left(\begin{array}{l}k^{0}_{f,A}\,\omega^{A}_{0,0}\\+k^{0}_{f,B}\,\omega^{B}_{0,0}\end{array}\right)\right\}\left(\frac{[M_A]}{[M_A]+[M_B]}\right)\\+\left(k_{trm,AA}\lambda^{A}_{0,0}+k_{trm,BA}\lambda^{B}_{0,0}\right)[M_A]\end{array}\right\}z$$
$$+k_{th}[M_A]^{3}(z+2z^{2})+\left(\frac{1}{2}\right)k^{0}_{f,A}\,[\omega^{A}_{0,0}\Omega^{A}_{0,0}(z,w)]$$
$$+(k_{p,AA}[\lambda^{A}_{0,0}\sigma^{A}_{0,0}(z,w)]+k_{p,AB}[\lambda^{B}_{0,0}\sigma^{B}_{0,0}(z,w)])[M_A]z$$
$$-\left\{\begin{array}{l}(k_{p,AA}+k_{trm,AA})[M_A]+(k_{p,AB}+k_{trm,AB})[M_B]\\+(k_{tc,AA}+k_{td,AA})\lambda^{A}_{0,0}+(k_{tc,AB}+k_{td,AB})\lambda^{B}_{0,0}\end{array}\right\}[\lambda^{A}_{0,0}\sigma^{A}_{0,0}(z,w)]$$
$$+\left(\frac{1}{2}\right)k_{f,A}\,([\gamma'^{AA}_{0,0}\Upsilon^{AA}_{0,0}(z,w)]+[\gamma'^{AB}_{0,0}\Upsilon^{AB}_{0,0}(z,w)])$$
$$-\left\{k_{a,A}(\omega^{A}_{0,0}+\omega^{B}_{0,0})+k^{0}_{a,A}[TR_0]\right\}[\lambda^{A}_{0,0}\sigma^{A}_{0,0}(z,w)]$$
$$-k_{c,A}\left(\begin{array}{l}\gamma'^{AA}_{0,0}+\gamma'^{AB}_{0,0}+\gamma'^{BB}_{0,0}\\+\omega^{A}_{0,0}+\omega^{B}_{0,0}\end{array}\right)\left\{\begin{array}{l}[\lambda^{A}_{0,0}\sigma^{A}_{0,0}(z,w)]\delta_{theory,IRT}+\\\left(\begin{array}{l}zw[R^{A}_{1,1}]+z[R^{A}_{1,0}]\\+z^{2}[R^{A}_{2,0}]\end{array}\right)\delta_{theory,IRTO}\end{array}\right\} \tag{A.19}$$

Pgf of order 0,0 of active radicals with a final unit of monomer B:

$$r_{\lambda^{B}_{0,0}\sigma^{B}_{0,0}}(z,w)=\left\{\begin{array}{l}\left\{2fk_{d}[I]+\left(\frac{1}{2}\right)\left(\begin{array}{l}k^{0}_{f,A}\,\omega^{A}_{0,0}\\+k^{0}_{f,B}\,\omega^{B}_{0,0}\end{array}\right)\right\}\left(\frac{[M_B]}{[M_A]+[M_B]}\right)\\+\left(k_{trm,AB}\lambda^{A}_{0,0}+k_{trm,BB}\lambda^{B}_{0,0}\right)[M_B]\end{array}\right\}w$$
$$+\left(k_{p,BA}[\lambda^{A}_{0,0}\sigma^{A}_{0,0}(z,w)]+k_{p,BB}[\lambda^{B}_{0,0}\sigma^{B}_{0,0}(z,w)]\right)[M_B]w$$
$$-\left\{\begin{array}{l}(k_{p,BB}+k_{trm,BB})[M_B]+(k_{p,BA}+k_{trm,BA})[M_A]\\+(k_{tc,BB}+k_{td,BB})\lambda^{B}_{0,0}+(k_{tc,BA}+k_{td,BA})\lambda^{A}_{0,0}\end{array}\right\}[\lambda^{B}_{0,0}\sigma^{B}_{0,0}(z,w)]$$
$$+\left(\frac{1}{2}\right)k_{f,B}\,([\gamma'^{BB}_{0,0}\Upsilon^{BB}_{0,0}(z,w)]+[\gamma'^{BA}_{0,0}\Upsilon^{BA}_{0,0}(z,w)])+\left(\frac{1}{2}\right)k^{0}_{f,B}\,[\omega^{B}_{0,0}\Omega^{B}_{0,0}(z,w)]$$
$$-\left\{k_{a,B}(\omega^{B}_{0,0}+\omega^{A}_{0,0})+k^{0}_{a,B}[TR_0]\right\}[\lambda^{B}_{0,0}\sigma^{B}_{0,0}(z,w)]$$
$$-k_{c,B}\left(\begin{array}{l}\gamma'^{AA}_{0,0}+\gamma'^{AB}_{0,0}+\gamma'^{BB}_{0,0}\\+\omega^{A}_{0,0}+\omega^{B}_{0,0}\end{array}\right)\left\{\begin{array}{l}[\lambda^{B}_{0,0}\sigma^{B}_{0,0}(z,w)]\delta_{theory,IRT}+\\\left(\begin{array}{l}zw[R^{B}_{1,1}]+w[R^{B}_{0,1}]\\+w^{2}[R^{B}_{0,2}]\end{array}\right)\delta_{theory,IRTO}\end{array}\right\} \tag{A.20}$$

Pgf of order 0,0 of one-arm dormant radicals with a final unit of monomer j (j = A, B*):*

$$r_{\mu^{j}_{0,0}\varphi^{j}_{0,0}}(z,w)=-(k_{a,i}\,\lambda^{i}_{0,0}+k_{a,j}\,\lambda^{j}_{0,0})[\mu^{j}_{0,0}\varphi^{j}_{0,0}(z,w)]$$
$$+\left(\frac{1}{2}\right)\left(k^{0}_{f,j}\,[\omega^{j}_{0,0}\Omega^{j}_{0,0}(z,w)]+k_{f,j}\,[\gamma'^{j,j}_{0,0}\Upsilon^{j,j}_{0,0}(z,w)]+k_{f,i}\,[\gamma'^{j,i}_{0,0}\Upsilon^{j,i}_{0,0}(z,w)]\right) \tag{A.21}$$

Pgf of order 0,0 of dead polymer radicals:

$$r_{\varepsilon_{0,0}\vartheta_{0,0}}(z,w)=\left(\begin{array}{l}k_{trm,AA}[M_A]+k_{trm,AB}[M_B]\\+k_{td,AA}\lambda^{A}_{0,0}+k_{td,AB}\lambda^{B}_{0,0}\end{array}\right)[\lambda^{A}_{0,0}\sigma^{A}_{0,0}(z,w)]$$
$$+\left(k_{trm,BA}[M_A]+k_{trm,BB}[M_B]+k_{td,BA}\lambda^{A}_{0,0}+k_{td,BB}\lambda^{B}_{0,0}\right)[\lambda^{B}_{0,0}\sigma^{B}_{0,0}(z,w)]$$
$$+k_{tc,AB}[\lambda^{A}_{0,0}\sigma^{A}_{0,0}(z,w)][\lambda^{B}_{0,0}\sigma^{B}_{0,0}(z,w)]$$
$$+\left(\frac{1}{2}\right)k_{tc,AA}[\lambda^{A}_{0,0}\sigma^{A}_{0,0}(z,w)]^{2}+\left(\frac{1}{2}\right)k_{tc,BB}[\lambda^{B}_{0,0}\sigma^{B}_{0,0}(z,w)]^{2}$$
$$+k_{c,A}\left(\begin{array}{l}[\theta^{AA}_{0,0}\Theta^{AA}_{0,0}(z,w)]+[\theta^{AB}_{0,0}\Theta^{AB}_{0,0}(z,w)]\\+[\theta^{BB}_{0,0}\Theta^{BB}_{0,0}(z,w)]+\\[\omega^{A}_{0,0}\Omega^{A}_{0,0}(z,w)]+[\omega^{B}_{0,0}\Omega^{B}_{0,0}(z,w)]\end{array}\right)\left\{\begin{array}{l}\lambda^{A}_{0,0}\delta_{theory,IRT}+\\\left(\begin{array}{l}zw[R^{A}_{1,1}]\\+z[R^{A}_{1,0}]+\\z^{2}[R^{A}_{2,0}]\end{array}\right)\delta_{theory,IRTO}\end{array}\right\}$$
$$+k_{c,B}\left(\begin{array}{l}[\theta^{AA}_{0,0}\Theta^{AA}_{0,0}(z,w)]+[\theta^{AB}_{0,0}\Theta^{AB}_{0,0}(z,w)]\\+[\theta^{BB}_{0,0}\Theta^{BB}_{0,0}(z,w)]+\\[\omega^{A}_{0,0}\Omega^{A}_{0,0}(z,w)]+[\omega^{B}_{0,0}\Omega^{B}_{0,0}(z,w)]\end{array}\right)\left\{\begin{array}{l}\lambda^{B}_{0,0}\delta_{theory,IRT}+\\\left(\begin{array}{l}zw[R^{B}_{1,1}]\\+w[R^{B}_{0,1}]+\\w^{2}[R^{B}_{0,2}]\end{array}\right)\delta_{theory,IRTO}\end{array}\right\} \tag{A.22}$$

Pgf of order 0,0 of two-arm adduct radicals in pre-equilibrium (one branch with 0 units in length) with a final unit of monomer j (j = A, B*):*

$$r_{\omega^{j}_{0,0}\Omega^{j}_{0,0}}(z,w)=k^{0}_{a,j}\,[TR_0]\,[\lambda^{j}_{0,0}\sigma^{j}_{0,0}(z,w)]-k^{0}_{f,j}\,[\omega^{j}_{0,0}\Omega^{j}_{0,0}(z,w)]$$
$$-\left(\begin{array}{l}k_{c,A}\,(\lambda^{A}_{0,0}\delta_{theory,IRT}+([R^{A}_{1,1}]+[R^{A}_{1,0}]+[R^{A}_{2,0}])\delta_{theory,IRTO})+\\k_{c,B}\,(\lambda^{B}_{0,0}\delta_{theory,IRT}+([R^{B}_{1,1}]+[R^{B}_{0,1}]+[R^{B}_{0,2}])\delta_{theory,IRTO})\end{array}\right)[\omega^{j}_{0,0}\Omega^{j}_{0,0}(z,w)] \tag{A.23}$$

Pgf of order 0,0 of the partial 0,0 order moment of two-arm adduct radicals with a final unit of monomer i in the first branch and a final unit of monomer j in the other branch (i, j = A, B*):*

$$r_{\gamma'^{i,j}_{0,0}\Upsilon^{i,j}_{0,0}}(z,w)=k_{a,i}\,\mu^{j}_{0,0}\,[\lambda^{i}_{0,0}\sigma^{i}_{0,0}(z,w)]+k_{a,j}\,\lambda^{j}_{0,0}\,[\mu^{i}_{0,0}\varphi^{j}_{0,0}(z,w)]$$
$$-\left(\frac{1}{2}\right)k_{f,i}\,[\gamma'^{i,j}_{0,0}\Upsilon^{i,j}_{0,0}(z,w)]-\left(\frac{1}{2}\right)k_{f,j}\,[\gamma'^{i,j}_{0,0}\Upsilon^{i,j}_{0,0}(z,w)]$$
$$-\left(\begin{array}{l}k_{c,A}\,(\lambda^{A}_{0,0}\delta_{theory,IRT}+([R^{A}_{1,1}]+[R^{A}_{1,0}]+[R^{A}_{2,0}])\delta_{theory,IRTO})+\\k_{c,B}\,(\lambda^{B}_{0,0}\delta_{theory,IRT}+([R^{B}_{1,1}]+[R^{B}_{0,1}]+[R^{B}_{0,2}])\delta_{theory,IRTO})\end{array}\right)[\gamma'^{i,j}_{0,0}\Upsilon^{i,j}_{0,0}(z,w)] \tag{A.24}$$

Pgf of order 0,0 of the two-arm adduct radicals with a final unit of monomer i in one branch and a final unit of monomer j in the other branch (i, j = A, B*), considering the total amount of units of each monomer (adding the units in both arms):*

$$r_{\theta^{i,j}_{0,0}\Theta^{i,j}_{0,0}}(z,w)=k_{a,i}\,[\mu^{j}_{0,0}\varphi^{j}_{0,0}(z,w)]\,[\lambda^{i}_{0,0}\sigma^{i}_{0,0}(z,w)]$$
$$+k_{a,j}\,[\lambda^{j}_{0,0}\sigma^{j}_{0,0}(z,w)]\,[\mu^{i}_{0,0}\varphi^{i}_{0,0}(z,w)]-\left(\frac{1}{2}\right)(k_{f,i}+k_{f,j})\,[\theta^{i,j}_{0,0}\Theta^{i,j}_{0,0}(z,w)]$$
$$-\left(\begin{array}{l}k_{c,A}\,(\lambda^{A}_{0,0}\delta_{theory,IRT}+([R^{A}_{1,1}]+[R^{A}_{1,0}]+[R^{A}_{2,0}])\delta_{theory,IRTO})+\\k_{c,B}\,(\lambda^{B}_{0,0}\delta_{theory,IRT}+([R^{B}_{1,1}]+[R^{B}_{0,1}]+[R^{B}_{0,2}])\delta_{theory,IRTO})\end{array}\right)[\theta^{i,j}_{0,0}\Theta^{i,j}_{0,0}(z,w)] \tag{A.25}$$

A.2. Kinetic parameters

The kinetic parameters that are not related with RAFT reactions were considered to be equal to those of the conventional free radical copolymerization of styrene and methyl methacrylate. These parameters are shown in Table A.1.

A.3. Density equations, average molecular properties, composition and conversion

The density equations used to compute the reaction volume are the following [59,60]:

$$\rho_{mix}=\left(\frac{x_{St}}{\rho_{St}}+\frac{x_{MMA}}{\rho_{MMA}}+\frac{x_{I}}{\rho_{I}}+\frac{x_{CTA}}{\rho_{CTA}}+\frac{x_{homoPSt}}{\rho_{homoPSt}}+\frac{x_{homoPMMA}}{\rho_{homoPMMA}}\right)^{-1} \tag{A.26}$$

$$\rho_{St}=919.3-0.665\cdot T(^{\circ}C)=\rho_{I}=\rho_{CTA};\ \rho_{MMA}=936-0.265\cdot T(^{\circ}C) \tag{A.27}$$

$$\rho_{homoPSt}=992.6-0.265\cdot T(^{\circ}C);\ \rho_{homoPMMA}=1190-0.265\cdot T(^{\circ}C) \tag{A.28}$$

In these expressions, ρ_{mix} is the density of the mixture while ρ_i and x_i represent the density and mass fraction of species i where i = St, MMA, I, CTA, poly(St) and poly(MMA). The mass fractions of species with low molecular weight are calculated according to the following equation:

$$x_i=\frac{[i]\ PM_i}{\rho_{mix}} \tag{A.29}$$

Table A.1
Kinetic parameter of the initiator decomposition, styrene thermal initiation, propagation, termination and transfer to monomer reactions for the free radical copolymerization of styrene (A) and methyl-methacrylate (B) [59].

Reaction	Parameter	Units
Initiation	$f = 0.62$	
	$k_d = 1.7 \times 10^{15} \exp\left(-\frac{30.000}{1.987 \cdot T}\right)$	s^{-1}
	$k_{th} = 2.19 \times 10^{4} \exp\left(\frac{-13.810}{T}\right)$	$L^2\ mol^{-2}\ s^{-1}$
Propagation	$k_{p,AA} = 4.27 \times 10^{7} \exp\left(\frac{-7769.17}{1.987 \cdot T}\right)$	$L\ mol^{-1}\ s^{-1}$
	$k_{p,BB} = 4.427 \times 10^{6} \exp\left(\frac{-6000}{1.987 \cdot T}\right)$	$L\ mol^{-1}\ s^{-1}$
	$rx_A = 0.57$	
	$rx_B = 0.41$	
	$k_{p,AB} = \frac{k_{p,AA}}{rx_A}$	$L\ mol^{-1}\ s^{-1}$
	$k_{p,BA} = \frac{k_{p,BB}}{rx_B}$	$L\ mol^{-1}\ s^{-1}$
Termination	$k_{tc,AA} = 3.05 \times 10^{-9} (k_{p,AA})^2 \exp\left(\frac{12452.2}{1.987 \cdot T}\right)$	$L\ mol^{-1}\ s^{-1}$
	$k_{tc,BB} = 0$	
	$k_{td,AA} = 0$	
	$k_{td,BB} = 9.8 \times 10^{7} \exp\left(\frac{-701}{1.987 \cdot T}\right)$	$L\ mol^{-1}\ s^{-1}$
	$k_{tc,AB} = (1 - f_{dc}) f_{i\ AB} \sqrt{k_{tc,AA} k_{td,BB}}$	$L\ mol^{-1}\ s^{-1}$
	$k_{td,AB} = f_{dc} f_{i\ AB} \sqrt{k_{tc,AA} k_{td,BB}}$	$L\ mol^{-1}\ s^{-1}$
	$f_{dc} = 0.5$	
	$f_{i\ AB} = 1.616$	
Chain transfer to monomer	$k_{trm,AA} = k_{p,AA} 0.22 \exp\left(\frac{-2820}{T}\right)$	$L\ mol^{-1}\ s^{-1}$
	$k_{trm,BB} = k_{p,BB}\ 5.15 \times 10^{-5}$	$L\ mol^{-1}\ s^{-1}$
	$k_{trm,AB} = k_{p,AB} \frac{k_{trm,BB}}{k_{p,BB}}$	$L\ mol^{-1}\ s^{-1}$
	$k_{trm,BA} = k_{p,BA} \frac{k_{trm,AA}}{k_{p,AA}}$	$L\ mol^{-1}\ s^{-1}$

To the best of our knowledge, no expression exists for the variation of the density of poly(St-*co*-AMS) with temperature. Therefore, an assumed fraction of each homopolymer in the copolymer chain needs to be calculated. The moments of order 1,0 account for the moles of styrene in the copolymer chains, while the moments of order 0,1 account for the moles of methyl methacrylate present in the copolymer. Therefore, the assumed mass fraction of poly(St) and poly(MMA) in the copolymer can be calculated by adding all the moments of order 1,0 and 0,1, respectively, as in the following equations:

$$x_{\text{homoP(St)}} = \frac{\left(\sum_h Moment^h_{1,0}\right) \text{PM}_{\text{St}}}{\rho_{mix}} \text{ and}$$
$$x_{\text{homoP(MMA)}} = \frac{\left(\sum_h Moment^h_{0,1}\right) \text{PM}_{\text{MMA}}}{\rho_{mix}} \tag{A.30}$$

In these expressions, the superscript h accounts for each polymeric species in the reaction medium, where h = active radicals, one-arm dormant radicals, two-arms dormant adduct radicals, and dead copolymer chains.

The average molecular properties of interest are calculated from the calculated moments, as follows:

Number-average molecular weight:

$$\overline{M_n} = \frac{\left(\sum_h Moment^h_{1,0}\right) \text{PM}_A + \left(\sum_h Moment^h_{0,1}\right) \text{PM}_B}{\left(\sum_h Moment^h_{0,0}\right)} \tag{A.31}$$

Weight-average molecular weight:

$$\overline{M_w} = \frac{\left(\sum_h Moment^h_{2,0}\right) (\text{PM}_A)^2 + \left(\sum_h Moment^h_{0,2}\right) (\text{PM}_B)^2 + 2 \left(\sum_h Moment^h_{1,1}\right) \text{PM}_A\ \text{PM}_B}{\left(\sum_h Moment^h_{1,0}\right) \text{PM}_A + \left(\sum_h Moment^h_{0,1}\right) \text{PM}_B} \tag{A.32}$$

where PM_i is the molecular weight of the comonomer i (i = A, B), and the superscript h accounts for each polymeric species in the reaction medium.

When calculating an average molecular weight for a given macromolecular species (that is, propagating radicals, dead chains, etc.), only the specific moments for this species must be included in the calculation instead of the sum of moments of all polymeric species.

The polydispersity index may be obtained from the calculated molecular weights.

Polydispersity index:

$$PDI = \frac{\overline{M_w}}{\overline{M_n}} \tag{A.33}$$

Molar fractions of a given species can also be calculated through the moments of order 0,0, since they account for the number of molecules of that species.

The equations to calculate different conversions are shown below:

Global Conversion:

$$Conv(\%) = \frac{\sum_h Moment^h_{1,0} + \sum_h Moment^h_{0,1}}{\sum_h Moment^h_{1,0} + \sum_h Moment^h_{0,1} + [\text{M}_A] + [\text{M}_B]}\ 100 \tag{A.34}$$

Monomer (A and B) conversions

$$Conv_A(\%) = \frac{\sum_h Moment^h_{1,0}}{\sum_h Moment^h_{1,0} + [\text{M}_A]}\ 100 \tag{A.35}$$

$$Conv_B(\%) = \frac{\sum_h Moment^h_{0,1}}{\sum_h Moment^h_{0,1} + [\text{M}_B]}\ 100 \tag{A.36}$$

Finally, the copolymer composition, expressed in terms of monomer A, is obtained through the moment values as follows:

Number-cumulative composition for the copolymer:

$$\overline{Comp_n} = \frac{\sum_h Moment^h_{1,0}}{\sum_h Moment^h_{1,0} + \sum_h Moment^h_{0,1}} \tag{A.37}$$

Number-instantaneous composition for the copolymer:

$$Comp\_Inst_A = \frac{k_{p,AA}[\text{M}_A]\lambda^A_{0,0} + k_{p,BA}[\text{M}_A]\lambda^B_{0,0}}{\left\{ \begin{array}{l} k_{p,AA}[\text{M}_A]\lambda^A_{0,0} + k_{p,BA}[\text{M}_A]\lambda^B_{0,0} + \\ k_{p,AB}[\text{M}_B]\lambda^A_{0,0} + k_{p,BB}[\text{M}_B]\lambda^B_{0,0} \end{array} \right\}} \tag{A.38}$$

References

[1] S. Grajales, Controlled Radical Polymerization Guide, Sigma-Aldrich Co. LLC. Materials Science, 2012.
[2] W.A. Braunecker, K. Matyjaszewski, Controlled/living radical polymerization: features, developments, and perspectives, Prog. Polym. Sci. 32 (2007) 93–146.
[3] M. Zhang, W.H. Ray, Modeling of "living" free-radical polymerization with RAFT chemistry, Ind. Eng. Chem. Res. 40 (2001) 4336–4352.
[4] H. Tobita, Fundamental molecular weight distribution of RAFT polymers, Macromol. React. Eng. 2 (2008) 371–381.
[5] K. Matyjaszewski, J. Spanswick, Controlled/living radical polymerization, Mater. Today 8 (2005) 26–33.
[6] C. Fortunatti, C. Sarmoria, A. Brandolin, M. Asteasuain, Prediction of the full molecular weight distribution in RAFT polymerization using probability generating functions, Comput. Chem. Eng. 66 (2014) 214–220.
[7] H. Tobita, On the discrimination of RAFT models using miniemulsion polymerization, Macromol. Theory Simul. 22 (2013) 399–409.
[8] G. Moad, Mechanism and kinetics of dithiobenzoate-mediated raft polymerization – status of the dilemma, Macromol. Chem. Phys. 215 (2014) 9–26.
[9] C. Barner-Kowollik, J.F. Quinn, T.L.U. Nguyen, J.P.A. Heuts, T.P. Davis, Kinetic investigations of reversible addition fragmentation chain transfer

polymerizations: cumyl phenyldithioacetate mediated homopolymerizations of styrene and methyl methacrylate, Macromolecules 34 (2001) 7849–7857.
[10] M.J. Monteiro, H. De Brouwer, Intermediate radical termination as the mechanism for retardation in reversible addition-fragmentation chain transfer polymerization, Macromolecules 34 (2001) 349–352.
[11] D. Konkolewicz, B.S. Hawkett, A. Gray-Weale, S. Perrier, RAFT polymerization kinetics: combination of apparently conflicting models, Macromolecules 41 (2008) 6400–6412.
[12] D. Konkolewicz, B.S. Hawkett, A. Gray-Weale, S. Perkier, Raft polymerization kinetics: how long are the cross-terminating oligomers?, J Polym. Sci., Part A: Polym. Chem. 47 (2009) 3455–3466.
[13] D. Konkolewicz, M. Siauw, A. Gray-Weale, B.S. Hawkett, S. Perrier, Obtaining kinetic information from the chain-length distribution of polymers produced by RAFT, J. Phys. Chem. B 113 (2009) 7086–7094.
[14] B. Klumperman, E.T.A. Van Den Dungen, J.P.A. Heuts, M.J. Monteiro, RAFT-mediated polymerization – a story of incompatible data?, Macromol Rapid Commun. 31 (2010) 1846–1862.
[15] M. Buback, O. Janssen, R. Oswald, S. Schmatz, P. Vana, A missing reaction step in dithiobenzoate-mediated RAFT polymerization, Macromol. Symp. 248 (2007) 158–167.
[16] A. Feldermann, M.L. Coote, M.H. Stenzel, T.P. Davis, C. Barner-Kowollik, Consistent experimental and theoretical evidence for long-lived intermediate radicals in living free radical polymerization, J. Am. Chem. Soc. 126 (2004) 15915–15923.
[17] M.J. Monteiro, Design strategies for controlling the molecular weight and rate using reversible addition-fragmentation chain transfer mediated living radical polymerization, J. Polym. Sci., Part A: Polym. Chem. 43 (2005) 3189–3204.
[18] Y. Kwak, A. Goto, Y. Tsujii, Y. Murata, K. Komatsu, T. Fukuda, A kinetic study on the rate retardation in radical polymerization of styrene with addition-fragmentation chain transfer, Macromolecules 35 (2002) 3026–3029.
[19] S.L. Brown, D. Konkolewicz, A. Gray-Weale, W.B. Motherwell, S. Perrier, Searching for stars: selective desulfurization and fluorescence spectroscopy as New tools in the search for cross termination side-products in RAFT polymerization, Aust. J. Chem. 62 (2009) 1533–1536.
[20] S.R.S. Ting, T.P. Davis, P.B. Zetterlund, Retardation in RAFT polymerization: does cross-termination occur with short radicals only?, Macromolecules 44 (2011) 4187–4193
[21] K. Suzuki, Y. Nishimura, Y. Kanematsu, Y. Masuda, S. Satoh, H. Tobita, Experimental validation of intermediate termination in RAFT polymerization with dithiobenzoate via comparison of miniemulsion and bulk polymerization rates, Macromol. React. Eng. 6 (2012) 17–23.
[22] I. Zapata-González, E. Saldívar-Guerra, J. Ortiz-Cisneros, Full molecular weight distribution in RAFT polymerization. New mechanistic insight by direct integration of the equations, Macromol. Theory Simul. 20 (2011) 370–388.
[23] R. Wang, Y. Luo, B.G. Li, S. Zhu, Modeling of branching and gelation in RAFT copolymerization of vinyl/divinyl systems, Macromolecules 42 (2009) 85–94.
[24] A. Zargar, F.J. Schork, Copolymer sequence distributions in controlled radical polymerization, Macromol. React. Eng. 3 (2009) 118–130.
[25] D. Wang, X. Li, W.J. Wang, X. Gong, B.G. Li, S. Zhu, Kinetics and modeling of semi-batch RAFT copolymerization with hyperbranching, Macromolecules 45 (2012) 28–38.
[26] M. Salami-Kalajahi, V. Haddadi-Asl, P. Ganjeh-Anzabi, M. Najafi, Dithioester-mediated RAFT polymerization: a kinetic study by mathematical modelling, Iran. Polym. J. 20 (2011) 459–478.
[27] P. Ganjeh-Anzabi, V. Hadadi-Asl, M. Salami-Kaljahi, H. Roghani-Mamaqani, A new approach for Monte Carlo simulation of RAFT polymerization, Iran. J. Chem. Chem. Eng. 31 (2012) 75–84.
[28] R. Wang, Y. Luo, B. Li, X. Sun, S. Zhu, Design and control of copolymer composition distribution in living radical polymerization using semi-batch feeding policies: a model simulation, Macromol. Theory Simul. 15 (2006) 356–368.
[29] Y. Ye, F.J. Schork, Modeling and control of sequence length distribution for controlled radical (RAFT) copolymerization, Ind. Eng. Chem. Res. 48 (2009) 10827–10839.
[30] X. Sun, Y. Luo, R. Wang, B.G. Li, B. Liu, S. Zhu, Programmed synthesis of copolymer with controlled chain composition distribution via semibatch RAFT copolymerization, Macromolecules 40 (2007) 849–859.
[31] X. Sun, Y. Luo, R. Wang, B.G. Li, S. Zhu, Semibatch RAFT polymerization for producing ST/BA copolymers with controlled gradient composition profiles, AIChE J. 54 (2008) 1073–1087.
[32] M.J. Monteiro, Modeling the molecular weight distribution of block copolymer formation in a reversible addition-fragmentation chain transfer mediated living radical polymerization, J. Polym. Sci., Part A: Polym. Chem. 43 (2005) 5643–5651.
[33] L. Hlalele, D.R. D'Hooge, C.J. Dürr, A. Kaiser, S. Brandau, C. Barner-Kowollik, RAFT-mediated ab initio emulsion copolymerization of 1,3-butadiene with acrylonitrile, Macromolecules 47 (2014) 2820–2829.
[34] G. Johnston-Hall, M.J. Monteiro, Kinetic modeling of "living" and conventional free radical polymerizations of methyl methacrylate in dilute and gel regimes, Macromolecules 40 (2007) 7171–7179.
[35] I. Zapata-González, E. Saldívar-Guerra, A. Flores-Tlacuahuac, E. Vivaldo-Lima, J. Ortiz-Cisneros, Efficient numerical integration of stiff differential equations in polymerisation reaction engineering: computational aspects and applications, Can. J. Chem. Eng. 90 (2012) 804–823.
[36] C. Barner-Kowollik, J.F. Quinn, D.R. Morsley, T.P. Davis, Modeling the reversible addition-fragmentation chain transfer process in cumyl dithiobenzoate-mediated styrene homopolymerizations: assessing rate coefficients for the addition-fragmentation equilibrium, J. Polym. Sci., Part A: Polym. Chem. 39 (2001) 1353–1365.
[37] H. Chaffey-Millar, M. Busch, T.P. Davis, M.H. Stenzel, C. Barner-Kowollik, Advanced computational strategies for modelling the evolution of full molecular weight distributions formed during multiarmed (star) polymerisations, Macromol. Theory Simul. 14 (2005) 143–157.
[38] C. Barner-Kowollik, T.P. Davis, M.H. Stenzel, Synthesis of star polymers using RAFT polymerization: what is possible?, Aust J. Chem. 59 (2006) 719–727.
[39] S.M. Jung, V.G. Gomes, Miniemulsion polymerisation via reversible addition fragmentation chain transfer in pseudo-bulk regime, Macromol. React. Eng. 5 (2011) 303–315.
[40] M. Drache, G. Schmidt-Naake, M. Buback, P. Vana, Modeling RAFT polymerization kinetics via Monte Carlo methods: cumyl dithiobenzoate mediated methyl acrylate polymerization, Polymer 46 (2005) 8483–8493.
[41] H. Chaffey-Millar, D. Stewart, M.M.T. Chakravarty, G. Keller, C. Barner-Kowollik, A parallelised high performance Monte Carlo simulation approach for complex polymerisation kinetics, Macromol. Theory Simul. 16 (2007) 575–592.
[42] E. Pintos, C. Sarmoria, A. Brandolin, M. Asteasuain, Modeling of RAFT polymerization processes using an efficient Monte Carlo algorithm in Julia, Ind. Eng. Chem. Res. 55 (2016) 8534–8547.
[43] C. Fortunatti, C. Sarmoria, A. Brandolin, M. Asteasuain, Prediction of the full molecular weight distribution in raft polymerization using probability generating functions, Comput. Aided Chem. Eng. 32 (2013) 859–864.
[44] G.S.W. Craig, C.J. Thode, M. Serdar Onses, P.F. Nealey, The use of block copolymers in nanoscale patterning, Mater. Matter. 6 (3) (2011) 82–85.
[45] U. Beginn, Gradient copolymers, Colloid Polym. Sci. 286 (2008) 1465–1474.
[46] C. Fortunatti, Ph.D. Thesis Simulación y Optimización de la Síntesis de Copolímeros de Estireno y Monómeros Acrílicos de Estructura Controlada, Universidad Nacional del Sur (Bahía Blanca, Buenos Aires, Argentina), 2015.
[47] K. Kubo, A. Goto, K. Sato, Y. Kwak, T. Fukuda, Kinetic study on reversible addition-fragmentation chain transfer (RAFT) process for block and random copolymerizations of styrene and methyl methacrylate, Polymer 46 (2005) 9762–9768.
[48] A.R. Wang, S. Zhu, Effects of diffusion-controlled radical reactions on RAFT polymerization, Macromol. Theory Simul. 12 (2003) 196–208.
[49] A.D. Peklak, A. Butté, G. Storti, M. Morbidelli, Gel effect in the bulk reversible addition-fragmentation chain transfer polymerization of methyl methacrylate: modeling and experiments, J. Polym. Sci., Part A: Polym. Chem. 44 (2006) 1071–1085.
[50] D.R. D'Hooge, M.F. Reyniers, G.B. Marin, The crucial role of diffusional limitations in controlled radical polymerization, Macromol. React. Eng. 7 (2013) 362–379.
[51] A. Brandolin, M. Asteasuain, Mathematical modeling of bivariate distributions of polymer properties using 2D probability generating functions. Part II: Transformation of population mass balances of polymer processes, Macromol. Theory Simul. 22 (2013) 273–308.
[52] M. Asteasuain, A. Brandolin, Mathematical modeling of bivariate polymer property distributions using 2D probability generating functions, 1 – Numerical inversion methods, Macromol. Theory Simul. 19 (2010) 342–359.
[53] gPROMS v3.7 – Model Developer Guide, Process Systems Enterprise Ltd., London, UK, 2013.
[54] C. Fortunatti, C. Sarmoria, A. Brandolin, M. Asteasuain, Theoretical analysis of nitroxide-mediated copolymerization of styrene and α-methyl-styrene under different operating policies and reactor designs, Macromol. React. Eng. 8 (2014) 260–281.
[55] R.X.E. Willemse, A.M. Van Herk, Copolymerization kinetics of methyl methacrylate-styrene obtained by PLP-MALDI-ToF-MS, J. Am. Chem. Soc. 128 (2006) 4471–4480.
[56] K.A. Davis, K. Matyjaszewski (Eds.), Statistical, Gradient, Block and Graft Copolymers by Controlled/Living Radical Polymerizations, Springer, Berlin, Germany, 2002.
[57] P.H.M. Van Steenberge, D.R. D'Hooge, Y. Wang, M. Zhong, M.F. Reyniers, D. Konkolewicz, K. Matyjaszewski, G.B. Marin, Linear gradient quality of ATRP copolymers, Macromolecules 45 (2012) 8519–8531.
[58] P.H.M. Van Steenberge, B. Verbraeken, M.F. Reyniers, R. Hoogenboom, D.R. D'Hooge, Model-based visualization and understanding of monomer sequence formation in gradient copoly(2-oxazoline)s on the basis of 2-methyl-2-oxazoline and 2-phenyl-2-oxazoline, Macromolecules 48 (2015) 7765–7773.
[59] M. Asteasuain, D. Covan, C. Sarmoria, A. Brandolin, C. Leite de Araujo, J.C. Pinto, 21st European Symposium on Computer Aided Process Engineering, vol. 29, Elsevier, 2011.
[60] Personal Communication from Prof. J.C. Pinto, Institute COPPE – Universidade Federal do Rio de Janeiro, 2007.